Long ant life span is maintained by a unique heat shock factor

Karl M. Glastad,[1,2] Julian Roessler,[3] Janko Gospocic,[1,2] Roberto Bonasio,[1,2] and Shelley L. Berger[1,2,3,4]

[1]Department of Cell and Developmental Biology, Perelman School of Medicine, University of Pennsylvania, Philadelphia, Pennsylvania 19104, USA; [2]Epigenetics Institute, Perelman School of Medicine, University of Pennsylvania, Philadelphia, Pennsylvania 19104, USA; [3]Department of Biology, School of Arts and Sciences, University of Pennsylvania, Philadelphia, Pennsylvania 19104, USA; [4]Department of Genetics, Perelman School of Medicine, University of Pennsylvania, Philadelphia, Pennsylvania 19104, USA

Eusocial insect reproductive females show strikingly longer life spans than nonreproductive female workers despite high genetic similarity. In the ant *Harpegnathos saltator* (*Hsal*), workers can transition to reproductive "gamergates," acquiring a fivefold prolonged life span by mechanisms that are poorly understood. We found that gamergates have elevated expression of heat shock response (HSR) genes in the absence of heat stress and enhanced survival with heat stress. This HSR gene elevation is driven in part by gamergate-specific up-regulation of the gene encoding a truncated form of a heat shock factor most similar to mammalian HSF2 (hsalHSF2). In workers, hsalHSF2 was bound to DNA only upon heat stress. In gamergates, hsalHSF2 bound to DNA even in the absence of heat stress and was localized to gamergate-biased HSR genes. Expression of hsalHSF2 in *Drosophila melanogaster* led to enhanced heat shock survival and extended life span in the absence of heat stress. Molecular characterization illuminated multiple parallels between long-lived flies and gamergates, underscoring the centrality of hsalHSF2 to extended ant life span. Hence, ant caste-specific heat stress resilience and extended longevity can be transferred to flies via hsalHSF2. These findings reinforce the critical role of proteostasis in health and aging and reveal novel mechanisms underlying facultative life span extension in ants.

[*Keywords*: proteostasis; longevity; aging; HSF; heat shock; *Harpegnathos saltator*; *Drosophila melanogaster*]

Supplemental material is available for this article.

Received November 11, 2022; revised version accepted May 9, 2023.

One of the most fascinating and pressing questions in biology relates to determinative factors of life span and potential extension of health span. Across metazoa, several conserved features of molecular aging occur as organisms reach the end of their natural life span: changes in the fidelity of genome and epigenome regulation, and accumulation of oxidative and proteome damage (Kaushik and Cuervo 2015; Labbadia and Morimoto 2015). Protein misfolding is a ubiquitous occurrence, and loss of proteostasis (the health of the proteome) with age has emerged as a major factor that leads to negative consequences of aging, with misfolded protein accumulation at end of life in many species (Taylor and Dillin 2011; Kaushik and Cuervo 2015). The taxonomic breadth of this aging phenotype is matched by an equivalently broad distribution and diversity of chaperone proteins that function to refold misfolded proteins (Kaushik and Cuervo 2015; Labbadia and Morimoto 2015). Furthermore, multiple studies point to up-regulation of chaperone proteins as a strategy for life span extension in mammals (Gifondorwa et al. 2007; Pérez et al. 2009; Salway et al. 2011), *D. melanogaster* (Wang et al. 2004; Vos et al. 2016), and *C. elegans* (Walker and Lithgow 2003).

Early understanding of proteostasis and chaperone function emerged from discovery of the classic heat shock response (HSR) (Lindquist 1986; Baler et al. 1993), an exceedingly rapid gene induction pathway. Central to the HSR are the heat shock transcription factors (HSFs), which are DNA binding proteins that activate transcription of numerous genes encoding chaperone proteins in response to proteomic insult. HSF1 is highly studied, and in basal non-heat-shock conditions HSF1 is typically sequestered in the cytoplasm as a monomer, bound to the chaperone HSP90 (among others). Upon proteomic insult, HSP90 disassociates from HSF1 monomers, which enter the nucleus, trimerize, and bind to and rapidly up-regulate HSR genes to oppose aggregation of misfolded proteins (Gomez-Pastor et al. 2018).

In mammals, multiple distinct HSF transcription factors exist and play distinct roles outside of this classical

Corresponding author: bergers@pennmedicine.upenn.edu
Article published online ahead of print. Article and publication date are online at http://www.genesdev.org/cgi/doi/10.1101/gad.350250.122.

mechanism of HSR gene induction. For example, in contrast to *HSF1*, which is ubiquitously expressed independent of heat stress, the *HSF1* paralog *HSF2* shows distinct tissue- and time point-specific expression patterns through mouse development (Gomez-Pastor et al. 2018). DNA binding and target gene induction show a more linear correlation with *HSF2* expression levels, compared with HSF1 (Gomez-Pastor et al. 2018). Furthermore, HSF2 interacts with HSF1, potentially overcoming cytoplasmic sequestration of HSF1 by HSP70/90, leading to HSR gene activation independent of proteomic insult via HSF1–HSF2 heterotrimers (Östling et al. 2007; Sandqvist et al. 2009; Åkerfelt et al. 2010). Hence, in mammals, HSR gene activation may be controlled outside of the context of heat shock via up-regulation of HSF2 levels.

Here we leveraged the natural plasticity in *Harpegnathos saltator* longevity to investigate the molecular regulation of life span. *H. saltator* workers can be naturally or experimentally induced to transition into reproductive status (termed "gamergates"), and through this process gain more than fivefold life span extension. We found that *H. saltator* gamergates possess a much higher resistance to heat stress compared with workers. Furthermore, even in the absence of heat stress, the transition from short-lived worker to long-lived gamergate results in increased gene expression of a truncated HSF most similar to human HSF2 (referred to here as hsalHSF2), which binds to genes encoding chaperones that are up-regulated in gamergates in the absence of heat stess. Ectopic expression of hsalHSF2 in the fly *Drosophila melanogaster* produces resilience to heat stress, extension of life span, and transcriptional changes similar to those observed in gamergates. Thus, we have linked the remarkable ant caste-specific extended longevity to the function of a specialized heat shock factor, hsalHSF2, and found that heat resilience and associated long life span can be transferred to flies via expression of this HSF.

Results

Gamergates show elevated expression of molecular chaperone genes in the absence of heat stress

Previous reports (Ghaninia et al. 2017) and our own observations indicated a striking difference in life span between normal workers and workers that have transitioned to gamergate status in *H. saltator*. We first investigated the molecular basis for this disparity via rigorous characterization of caste life span using multiple colonies under identical conditions. Observations of worker survival from across >40 colonies (see the Materials and Methods for details; Supplemental Table S1) confirmed that worker survival suffered precipitous reduction over 220–280 d (7–9 mo) of age (Fig. 1A, left), whereas gamergate survival was constant over 8–24 m of age (Fig. 1A, right).

To uncover the molecular basis for this remarkable inducible life span extension, we performed RNA-seq in brains and fat bodies from young (d40) and old ants. We used older workers of 220–235 d, corresponding to the end of life of workers (Fig. 1B), whereas older gamergates were represented by samples of both d220–d235 ($n = 5$) and ≥1 yr old (n = 6) (see the Materials and Methods). We examined brain tissue given our prior work studying behavior in this species (Gospocic et al. 2017, 2021; Sheng et al. 2020) and owing to the strong link between aging and neurodegeneration in many organisms (Dukay et al. 2019). Fat body was used due to multiple functions related to aging (liver-like tissue having metabolic and energy homeostasis functions) and its relatively simple structure (Arrese and Soulages 2010).

In both tissues, we identified genes significantly differing between castes, as well as genes showing preferential increase or decrease in one caste relative to the other with increased age. This identified genes generally biased to one caste, as well as genes showing caste-specific change with age. Among differentially expressed genes (DEGs) between castes, as well as genes showing caste-specific changes in expression with age, we noted enrichment of multiple functional terms reflecting differential expression of DNA repair pathways, telomere maintenance, metabolism, and immune function; these terms appear to reflect the differential aging between castes (Supplemental Table S2). We evaluated conserved patterns in caste-biased gene expression between the two tissues and observed enrichment of functions related to proteostasis and chaperone activity among DEGs in both tissues. Noteably, these genes were either biased in expression to gamergate, increased in gamergates relative to workers with increased age, or decreased in workers relative to gamergates with age (Fig. 1B; Supplemental Fig. S1A).

Prior work has shown a strong link between proteostasis breakdown and negative consequences of aging (Kaushik and Cuervo 2015), and a major component of stress-related mortality is the aggregation of misfolded proteins (Soti and Csermely 2003; Taylor and Dillin 2011), which is thwarted by chaperone proteins (Zhang and Cuervo 2008; Calderwood et al. 2009; Morrow and Tanguay 2015). Hence, we closely examined DEGs related to chaperone function and management of misfolded proteins and found numerous genes expressed at higher levels in old gamergates relative to old workers in both tissues (Fig. 1C; Supplemental Fig. S1A,B; Supplemental Table S3), consistent with the functional enrichment pathways above (Fig. 1B). Indeed, among well-known chaperone genes conserved between ants and mammals (Supplemental Table S3), we found 22 that were significantly more highly expressed in at least one tissue in old gamergates (Fig. 1C; Supplemental Fig. S1B,C; Supplemental Table S3); 17 genes showed significantly higher expression in fat bodies from old gamergates, and 14 genes showed significantly higher expression in brains (Fig. 1C; Supplemental Fig. S1B,C), with nine genes showing consistent bias to old gamergates in both the brain and fat body (the top eight are shown in Fig. 1C). Interestingly, in brains, a pattern of worker gene expression decreasing with age was more apparent (Fig. 1C; Supplemental Fig. S1B), while in fat body, there was a stronger signal of either general gene expression bias to gamergates or gene expression bias to old gamergates (relative to old workers) (Fig. 1C; Supplemental Fig. S1C). These genes included HSP

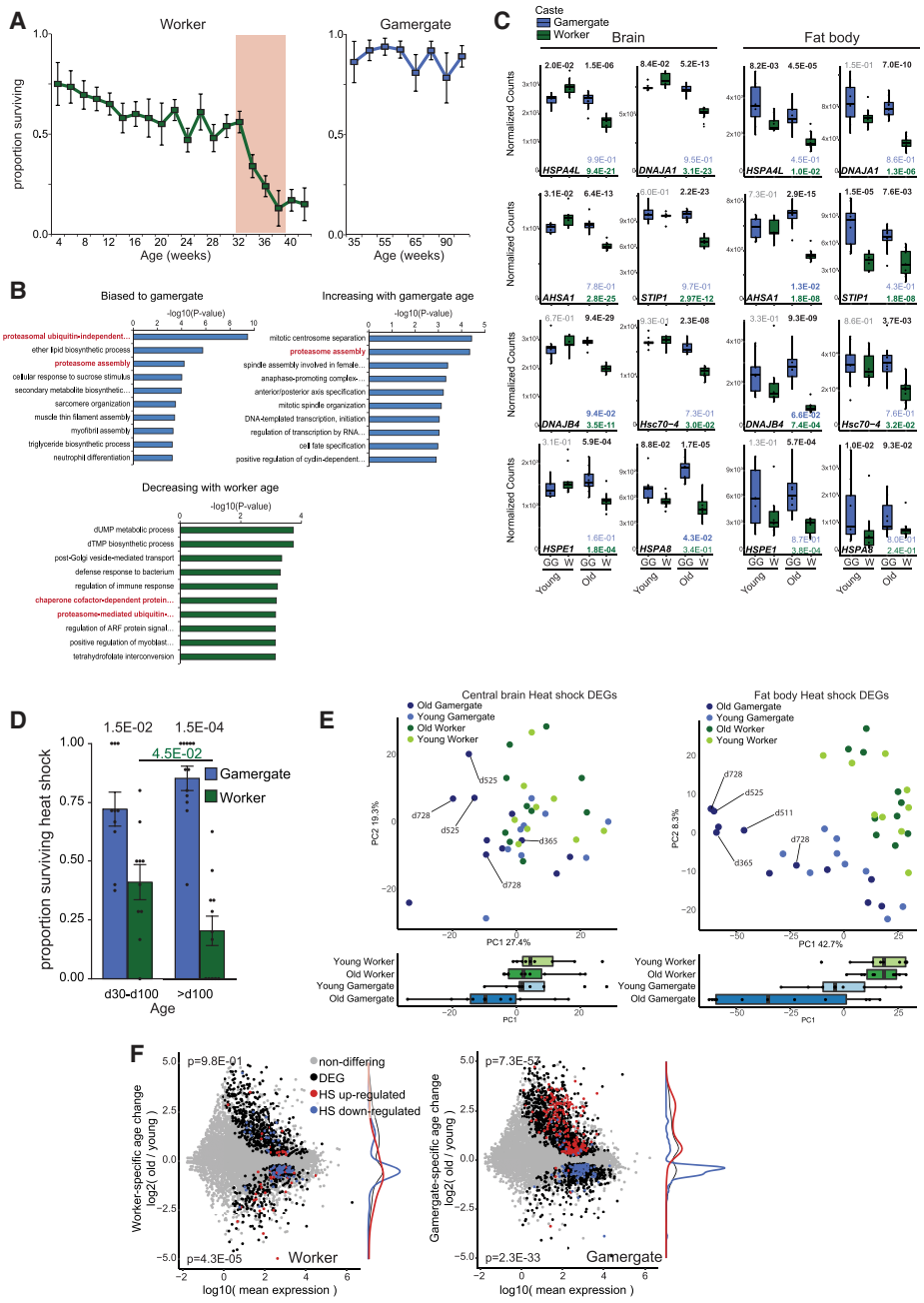

Figure 1. Enhanced heat shock survival in gamergates. (*A*) Life span of workers and gamergates. Worker data represent cohorots of ants painted each week and censused after 1 yr, and then repeated 2 mo later. Gamergate data represent wire-tagged foundational gamergates from the same colonies. Worker and gamergate data represent $n \geq 25$ for each age (Supplemental Table S1). (*B*) Gene ontology term (biological process) results for the top 10 terms enriched among genes significantly biased in expression to gamergates (*top left*), showing significant increase in expression as gamergates age relative to workers (*top right*), and showing significant decrease in workers relative to gamergates with age (*bottom*), illustrating enrichment of proteome- and chaperone-related terms in these categories (denoted by red text). Shown are gene ontology terms enriched among RNA-seq data originating from the fat body. For equivalent results from the brain, see Supplemental Figure S1A. (*C*) RNA-seq count plots (normalized counts) illustrating multiple HSPs/HSCs more highly expressed in GGs without heat shock, particularly in older gamergates. *P*-values represent adjusted *P*-values from DESeq2. *P*-values shown in green and blue represent significance testing of age-associated changes in gene expression biased to a given caste, with green representing worker-biased decrease in expression with age and blue representing gamergate-biased increase in expression with age. For aging RNA-seq, $n \geq 9$ for each caste X age (Supplemental Table S16). (*D*) Survival upon prolonged heat shock (18 h at 36.5°C) for gamergates (blue) and workers (green) of two age groups, illustrating that gamergates show significantly greater survival after heat shock, while workers show age-associated decline in survival. Above d100: $n = 12$; d30–d100: $n = 10$. *P*-values from a Mann–Whitney *U* test. The *P*-value shown in green represents significance of difference between d30 and d100 and over d100 worker survival. (*E*) Principle component analysis of aging RNA-seq samples using genes significantly up-regulated upon heat shock, comparing data from brains (*left*) and fat body (*right*), illustrating that genes up-regulated upon heat shock segregate gamergates and workers (blue and green, respectively), as well as old gamergates from young gamergates (dark and light blue, respectively). For samples from gamergates of ages ≥1 yr, specific age of given samples is indicated. (*F*) MA plots of genes showing caste-specific age-related changes in expression in fat body (for the brain, see Supplemental Fig. S1C), with 1-h HS up-regulated and HS down-regulated genes colored in red and blue, respectively. *P*-values at the the *top* and *bottom* are from a Fisher's exact test comparing up-regulated and down-regulated caste-biased age-changing genes with 1-h heat shock up-regulated and down-regulated DEGs, respectively. (HS) Heat shock.

and DNAJ and α-crystallin proteins, which have central roles as molecular chaperones to manage protein folding and misfolding (Qiu et al. 2006; Vos et al. 2008).

Gamergates are resistant to heat stress but show a blunted heat shock response

Thus, because chaperone genes show natural up-regulation in old gamergates, we assessed whether gamergates have increased survival under proteomic stress. Indeed, we found gamergates were notably resistant to heat stress compared with workers (~70% vs. ~40% survival; d30–d100: $P = 1.5 \times 10^{-2}$; over d100: $P = 1.5 \times 10^{-4}$) (Fig. 1D; Supplemental Table S4). Moreover, gamergate survival following heat stress remained constant between younger and older individuals, whereas older workers exhibited a pronounced twofold decrease in survival (~20%) relative to younger workers (~40%; $P = 4.50 \times 10^{-2}$) (Fig. 1D). This pattern remained with subsetting these data into 30-d increments, with a progressive decrease in worker survival with the approach to end of life compared with constant survival of gamergates (over d150; d120–d150:$P = 2.1 \times 10^{-2}$; d150–d180: $P = 4.1 \times 10^{-2}$; over d180: $P = 1.7 \times 10^{-2}$) (Supplemental Fig. S1D).

To uncover the molecular basis of this enhanced survival of gamergates under heat stress, we performed RNA-seq of central brains (Ito et al. 2014) and fat body from aged workers and gamergates following 1 h of heat stress (40°C). We harvested tissues from 220- to 260-d-old age-matched workers and gamergates, which is the upper limit of worker life span (Fig. 1A, shaded area); we thus maintained constant age for this comparison between workers and gamergates despite the longer life span of gamergates.

We examined the general transcriptome response to 1 h of heat stress via pooling data from both castes. Following heat stress, we detected 1425 differentially expressed genes (DEGs) in the fat body (771 up-regulated and 663 down-regulated) (Supplemental Fig. S3A, top panels) and 4092 DEGs in the brain (2162 up-regulated and 1930 down-regulated) (Supplemental Fig. S3B, top panels; Supplemental Table S5). The larger number of DEGs detected in the brain is notable because neurons in mammals show a blunted HSR relative to other tissues (San Gil et al. 2017), which may manifest as a stronger proteomic insult in both castes upon heat stress, resulting in a greater global transcriptomic response. This was supported by enrichment of functional terms associated with apoptosis, oxidative stress, and hypoxia response among genes up-regulated by heat stress in the brain that are not up-regulated in fat body (1689 genes) (Supplemental Table S6). Nevertheless, in both tissues, functional terms associated with up-regulated genes indicated an immediate HSR to the heat stress insult, including terms related to protein folding, chaperone activity and rapid transcriptional response. Down-regulated genes indicated more diverse organismal and cellular functions, including mRNA processing and translation machinery (Supplemental Fig. S3A,B, top panels; Supplemental Table S6), as predicted for shutdown of normal physiology.

We next assessed caste-specific responses to the 1-h heat stress in both tissues to understand the disparate heat stress survival between castes. We identified DEGs showing significantly stronger up-regulation or down-regulation in one caste upon heat stress relative to the other caste (see the Materials and Methods). Surprisingly, despite markedly better survival following heat stress, there were considerably fewer genes showing gamergate-specific transcriptional response compared with workers (brains: 803 gamergate-specific DEGs vs. 1188 worker-specific DEGs; fat body: 91 gamergate-specific DEGs vs. 716 worker-specific DEGs) (Supplemental Fig. S3A,B, bottom panels). In fat body, gamergate-specific up-regulated DEGs after heat stress showed functional enrichment of terms associated with various functions not overtly related to a response to heat shock (Supplemental Fig. S3A, bottom panels; Supplemental Table S5); in contrast, worker-specific DEGs after heat stress showed top terms similar to general DEGs after heat stress (in both castes), including "protein refolding," molecular chaperone-related terms, and "response to heat" (Supplemental Fig. S3A, middle panels). In brains, gamergate-specific up-regulated DEGs following heat stress showed functional enrichment associated with protein translation as well as HSR (Supplemental Fig. S3B, bottom panels; Supplemental Table S6), whereas worker-specific DEGs after heat stress showed stronger enrichment of general HSR pathways (Supplemental Fig. S2B, middle panels). These results indicate that immediately following heat stress, workers, not gamergates, preferentially and more strongly up-regulate genes in both tissues related to immediate stress response (including the HSR). We hypothesized that the blunted gene up-regulation in stressed gamergates may be due to the constitutively elevated levels of many chaperone proteins in normal gamergates noted above (Fig. 1B,C).

To assess this, we compared heat stress RNA-seq with the natural aging RNA-seq. We performed PCA on the natural aging data and then assessed whether genes up-regulated upon heat stress segregated gamergates and workers during aging. In fat body, heat stress up-regulated genes strongly segregated the transcriptome of natural aged workers and gamergates (Fig. 1E, right), showing that heat stress DEGs vary in expression in a caste-specific manner. While this pattern of genes responding to heat stress segregating aging caste was less pronounced in brains (Fig. 1E, left), strikingly, in both tissues, older gamergates very strongly segregated on the PCA, while older workers did not (Fig. 1E; Supplemental Fig. S3C). These results indicate that both gamergate status and gamergate age are associated with genes differentially regulated in response to heat stress.

We then directly compared age-associated DEGs of natural castes with DEGs upon heat stress. Consistent with our hypothesis, in fat body from unstressed old gamergates, genes activated in response to heat stress were up-regulated (Fig. 1F, right, red points), and genes deactivated in response to heat stress were down-regulated (Fig. 1F, right, blue points); a similar correlation was observed in gamergate brains, although not quite as strong (Supplemental Fig. S4A, bottom). Importantly, this

correlation was not found in either tissue for the workers (Fig. 1E, left), and indeed, in worker brains, the opposite was the case, where genes associated with the heat stress response were overall down-regulated with age (Supplemental Fig. S4A, top).

In summary, in both brains and fat body, aging gamergates up-regulate or maintain a HSR gene expression program, a pattern that is particularly clear in fat body. Importantly, in both tissues, aging workers down-regulate heat stress and protein folding genes, while aging gamergates do not (Fig. 1B,C; Supplemental Fig. S3A). These changes in gene expression in untreated gamergates provide a potential molecular basis for enhanced heat stress resilience compared with workers (Fig. 1D; Supplemental Fig. S1D) and, potentially, long life span of gamergates relative to workers.

hsal*HSF2 shows gamergate-biased expression without heat shock*

We sought to understand whether transcriptional regulators might drive this remarkable pattern of up-regulation of HSR genes in old gamergates. Heat shock factors (HSFs) are a family of DNA binding transcription factors that up-regulate HSR genes encoding heat shock proteins (HSPs), including molecular chaperones that participate in the classic heat shock pathways as well as in the response to other stressors. We uncovered an HSF transcription factor paralog in *H. saltator* that does not exist in *D. melanogaster*. This HSF gene (NCIB ID: *LOC10518 4310*) was markedly up-regulated by aging gamergates in both fat body and brains, whereas its expression either remained low (in fat body) or further decreased (in brains) in aging workers (Fig. 2A). We aligned the protein sequence and its paralog, *hsal*HSF1 (which was expressed at constitutively high levels in all samples but slightly elevated in young gamergates) (Fig. 2A, left), to sequences for all three characterized *Homo sapiens* HSF proteins. This revealed similarity to human HSF2 (Fig. 2B), and we therefore named this newly described protein hsalHSF2. Mammalian HSF2 is an unusual HSF transcription factor: While it has no reported function in life span determination, it has a heat shock-independent role during development and up-regulates HSR genes similarly to HSF1 (Åkerfelt et al. 2010), although independent of direct heat insult (Östling et al. 2007). Hence, hsalHSF2 may activate stress response genes in gamergates independent of the classical HSR pathway. Curiously, hsalHSF2 is a truncated form of typical HSFs, maintaining an intact DNA binding domain but lacking the TAD (transcriptional activation domain) and RD (regulatory domain). hsalHSF2 includes a partial oligomerization domain (HR-A/B) (Fig. 2B, bottom); however, given the low conservation of HR-A/B, it is unclear whether hsalHSF2 would be able to trimerize with HSFs. *hsalHSF2* has gene paralogs in all *Hymenopteran* species, illustrating evolutionary conservation across eusocial and noneusocial species (Supplemental Fig. S4B). Examination of all insect genomes on orthoDB (Waterhouse et al. 2011) identified truncated *HSF2* in many holometabola, in locusts (*Locusta migratoria*, Polyneoptera), and in *Pediculus humanus* (Psocodea), suggesting its presence in ancestral insects but repeated loss in multiple major groups (Supplemental Fig. S4C). Hence, *hsalHSF2* paralogs occur in many noneusocial species lacking facultative life span extension. To gain a more comprehensive overview, we used RT-qPCR to profile *hsalHSF2* expression during *H. saltator* developmental stages, in other tissues in aged workers and gamergates and in young workers and gamergates. *hsalHSF2* has its highest relative expression in early embryos (eggs <4 d old) (Supplemental Fig. S5A, left) and thus is similar to the highest mouse HSF2 expression in early embryonic stages (Mezger et al. 1994) and in chickens (Kawazoe et al. 1999), supporting functional similarity between hsalHSF2 and HSF2 in mammals. In aged ant tissues, *hsalHSF2* maintained strong gamergate-biased expression in brains and fat body, was elevated in gamergate ovaries ($P = 3.3 \times 10^{-3}$), and trended higher in gamergates in the mandibular gland ($P = 7.4 \times 10^{-2}$) (Supplemental Fig. S5A, middle). Compared with young workers, young gamergates showed significantly higher *hsal*HSF2 expression in fat body ($P = 1.6 \times 10^{-3}$) and ovaries ($P = 5.0 \times 10^{-5}$) but not in brains (Supplemental Fig. S5A, right), supporting trends in fat body via RNA-seq (Fig. 2A).

HSF2 binds genes in gamergates without heat stress

To explore whether hsalHSF2 specifically activates HSR genes in gamergates, we developed specific antibodies to *H. saltator* hsalHSF1 and to hsalHSF2 (Supplemental Fig. S5B). We observed elevated hsalHSF2 protein without heat stress in old gamergates relative to old workers (Supplemental Fig. S5B), similar to RNA (Fig. 2A). We performed ChIP-seq of hsalHSF1 and hsalHSF2 in gamergates and workers with and without stress using age-matched old ants (d220–d260) as for the heat shock RNA-seq experiments (Supplemental Fig. S5). There was binding of both hsalHSF1 and hsalHSF2 in fat body and brains with heat stress (Supplemental Fig. S5C), as expected given roles in mediating the HSR. hsalHSF1 bound to >7000 sites upon heat stress, and hsalHSF2 bound to 2612 sites (Supplemental Fig. S5C). The majority of sites bound by hsalHSF2 upon heat stress were also bound by hsalHSF1, with hsalHSF1 targeting more genes than hsalHSF2 (Supplemental Table S7; Supplemental Fig. S5C,D). Genes bound by hsalHSF1 and hsalHSF2 during heat stress were characterized by functional terms related to translation, protein folding, and heat response (Supplemental Table S8).

Strikingly, in contrast to workers, we found far more sites in gamergates bound by hsalHSF2 in the absence of heat stress (Supplemental Fig. S5C,D), consistent with the hypothesis that hsalHSF2 acts in a heat-stress-independent manner, as observed in mammals (Östling et al. 2007). Without heat stress, genes bound by hsalHSF2 in gamergates showed much less overlap with hsalHSF1 binding (Supplemental Fig. S5D, middle). Nevertheless, hsalHSF2 showed increased binding with heat stress in both castes, and this was associated with up-regulation of hsalHSF2 transcription upon heat shock (Supplemental Fig. S5E). In summary, HSF1 functions similarly in

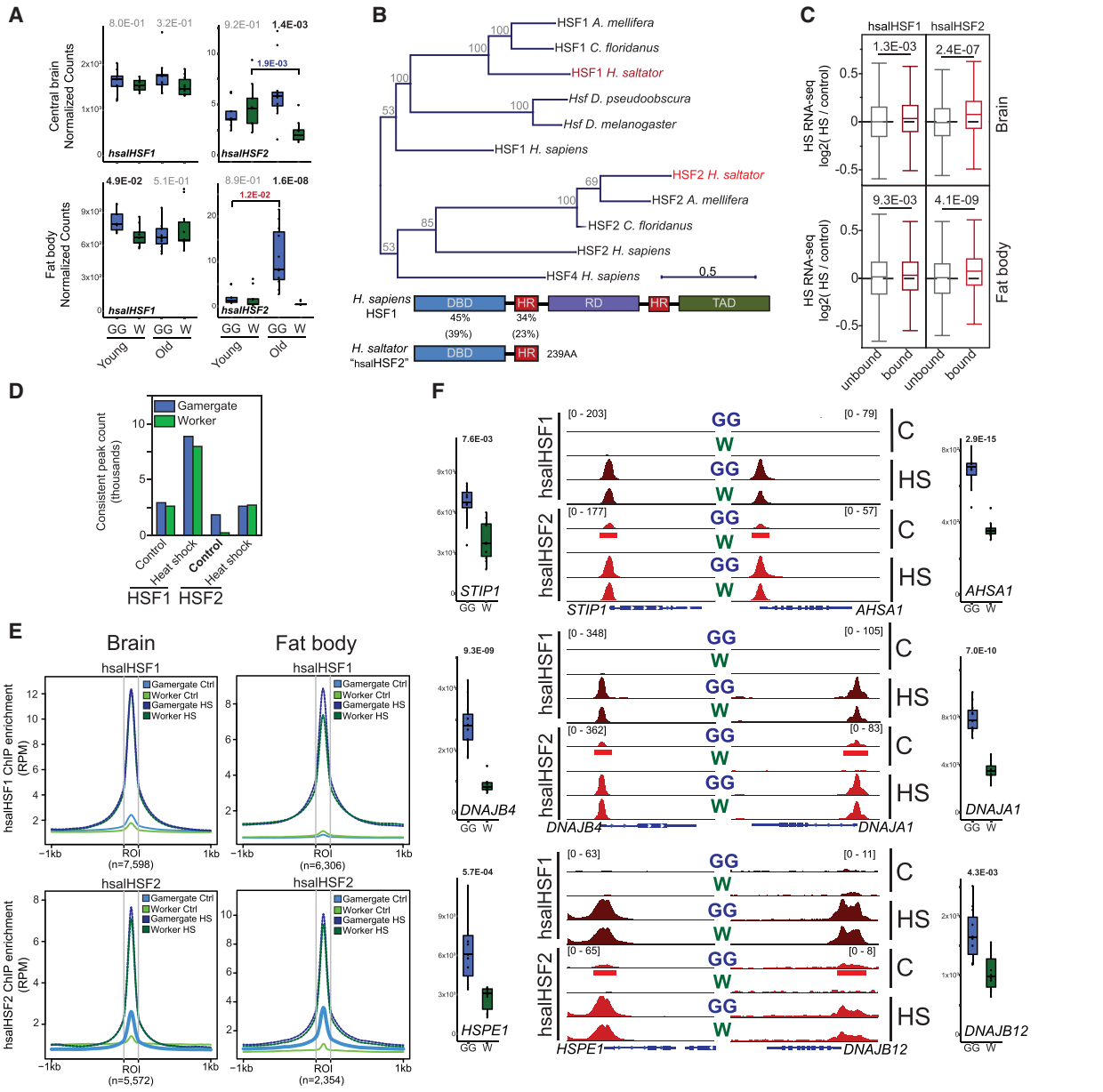

Figure 2. *hsalHSF2* shows gamergate-biased expression and non-heat-shock binding. (*A*) Normalized counts for HSF1 (*left*) and *hsalHSF2* (*right*) in *H. saltator* young and old workers and gamergates for brains (*top*) and fat body (*bottom*), showing gamergate-biased expression of *hsalHSF2* in older ants. *P*-values represent adjusted *P*-values taken from DESeq2. For *hsalHSF2* genes showing age-related decline (blue *P*-values) or age-related increase (red *P*-values) in expression, *P*-values are given when significant. (GG) Gamergate, (W) worker. (*B*) Protein alignment (PRANK on protein sequences) phylogenetic tree illustrating that *hsalHSF2* is closer to *H. sapiens* HSF2 relative to HSF1 and HSF4. Numbers shown at nodes represent bootstrap values after 1000 iterations. *Below* is a schematic of *H. sapiens* HSF1 as compared with *H. saltator hsal*HSF2, with percent AA conservation shown between respective domains (parenthetical values represent percent conservation as compared with *D. melanogaster Hsf*). (*C*) *hsalHSF2* (light red) is more predictive of heat shock up-regulation of gene expression than *hsalHSF1* (dark red) in both brains (*top*) and fat body (*bottom*). *P*-values from a Mann–Whitney *U*-test comparing genes lacking HSF binding with those possessing it. (*D*) Number of peaks detected in data from fat body for hsalHSF1 and hsalHSF2 in workers and gamergates, illustrating very low peak count for hsalHSF2 in workers without heat shock (control), while non-heat-shocked gamergates show similar numbers of peaks with and without heat shock. (*E*) Meta-plots of normalized ChIP-seq signal (reads per million [RPM], averaged across three replicates) for HSFs at peaks generally bound by the respective HSF upon heat shock, showing that hsalHSF2 (*right*) shows binding in gamergates only (light blue) without heat shock at loci bound by hsalHSF2 upon heat shock (irrespective of caste). (*F*) Example genome browser tracks for six genes shown in Figure 1F illustrating binding by hsalHSF2 in gamergates in the absence of heat shock (red underlined peaks represent significantly gamergate-biased peaks; FDR < 0.05). For respective HSFs, all tracks were autoscaled to one another (RPM values are in brackets). (C) Control, (HS) heat shock, (GG) gamergate samples, (W) worker samples. Beside each track is shown the count plots representing old caste untreated RNA-seq (as shown in Fig. 1F). *P*-values in count plots represent adjusted *P*-values from DESeq2.

gamergates and workers in heat stress conditions, whereas in non-heat-stress basal conditions, hsalHSF2 (which is preferentially expressed in old gamergates) shows strong binding exclusively in gamergates.

We examined the overall role of hsalHSF1 and hsalHSF2 in binding during the heat stress transcriptional response. Surprisingly, when comparing HSF ChIP-seq binding with heat stress RNA-seq, we found that hsalHSF2 binding was more predictive of general heat stress up-regulation of gene expression for both brains (Fig. 2C, top) and fat body (Fig. 2C, bottom) RNA-seq. We also found hsalHSF2 enrichment level was also more strongly correlated with level of heat stress gene induction (although hsalHSF1 was also predictive of heat stress gene up-regulation) (Supplemental Fig. S5F,G). Because hsalHSF1 binds the majority of loci bound by hsalHSF2, this stronger correlation between hsalHSF2 and heat stress up-regulation may be due to hsalHSF2 showing more specificity to direct the up-regulation of heat stress genes. In support of this, correlations between heat stress gene expression change and hsalHSF1 peak enrichment were stronger when considering only genes also marked with hsalHSF2 (Supplemental Fig. S5G, right). This suggests that hsalHSF1 is more permissive in its binding, including binding to either genes showing weaker heat stress response or genes that are repressed upon heat stress, as seen in other systems (Xie and Calderwood 2001).

For non-heat-stressed conditions, we observed a striking difference in hsalHSF2 ChIP-seq peak counts in gamergates compared with workers (Fig. 2D; Supplemental Fig. S5C). Notably, hsalHSF2 showed marked binding in gamergates without heat stress in both tissues (Fig. 2E, bottom, thick blue line; Supplemental Fig. S6A [bottom], B) but much less or no binding in workers without heat stress (Fig. 2E, bottom, thin green line; Supplemental Fig. S6A [bottom], B). Thus, hsalHSF2 binding without heat stress may up-regulate HSR genes in aging gamergates, and this may be central to long life span in gamergates. To assess this, we examined the cohort of naturally gamergate-biased HSR genes/chaperone protein genes (Fig. 1C; Supplemental Fig. S1B,C) for binding of hsalHSF2 without heat stress. We found that 15 out of 22 of these genes showed gamergate-specific hsalHSF2 binding in the absence of heat stress in the same tissue showing elevated gene expression in gamergates without heat stress (10 out of 14 in brains and 13 out of 17 in fat body) (six in Fig. 2F; six in Supplemental Fig. S7A,B, brain; Supplemental Table S3), and these same genes displayed robust binding of both hsalHSF1 and hsalHSF2 in both castes upon heat stress (Fig. 2F; Supplemental Fig. S7A,B). Indeed, the majority of DNA sites bound by hsalHSF2 in unstressed gamergates became much more highly bound in both castes with heat stress (Fig. 2E; Supplemental Fig. S6A, B), implying that non-heat-stress hsalHSF2 binding to genes operates under the same principles as with heat stress; however, binding in the absence of heat stress is restricted to gamergates.

As expected, genes showing binding of hsalHSF2 in gamergates at normal temperature also tended to be up-regulated in gamergates compared with workers (fat body shown in Supplemental Fig. S7C,D, brains). This moderate bias is likely because hsalHSF2 is not the major driver of caste-specfic differential gene expression (Gospocic et al. 2021); instead, we propose that hsalHSF2 mediates up-regulation of gamergate gene expression in the basal condition for a subset of stress response genes, and this is supported by the observation that the magnitude of hsalHSF2 association is considerably higher when limited to genes showing heat stress induction in our data (Fig. 3A, fat body). Indeed, among the 216 genes showing general gamergate bias and also featuring a non-heat-stress hsalHSF2 peak, the functional categories most enriched were associated with HSR or unfolded protein binding (Supplemental Table S8).

We then examined whether genes that had hsalHSF2 binding in gamergates without heat stress correlated with increased gene expression in old gamergates. We found that in both tissues (upon subsetting our data to genes showing general decline in our aging data irrespective of caste), hsalHSF2 gamergate-bound genes (1) were more biased to old gamergates (Fig. 3B, top) and (2) showed increased expression (relative to unbound genes) as gamergates aged (Fig. 3B, middle), but (3) showed either decreased expression or no change as workers aged (Fig. 3B, bottom). This suggests that hsalHSF2 participates in the basal activation of the HSR at normal temepratures in aging gamergates, consistent with the patterns of *hsalHSF2* expression (Fig. 2A).

We examined whether hsalHSF2-bound genes are more predictive of the association between heat stress gene expression and bias to gamergate expression (Fig. 1). Indeed, at heat stress DEGs, genes bound by hsalHSF2 in gamergates without heat stress showed a much stronger association between heat shock differential regulation and biased expression to old gamergates (Fig. 3C). Specifically, genes bound in gamergates without heat stress by hsalHSF2 are more likely to show both heat stress up-regulation and expression bias to old gamergates without heat stress (Fig. 3C, red points). This further supports our hypothesis that the observed association between basal gene expression bias to gamergates and heat stress differential expression is driven in part by *hsal*HSF2 binding in gamergates without heat stess.

We further note that, for many core chaperone genes (e.g., Fig. 1C; Supplemental Fig. S1B,C) showing biased expression to old gamergates, *hsalHSF2* expression levels (Fig. 2A) track chaperone levels. In the fat body, *hsalHSF2* is more highly expressed in old gamergates (relative to all other samples), and chaperone genes show a similar pattern of increased expression in old gamergates, while, in brains, *hsalHSF2* decreased in expression for old workers, paralleling decreased chaperone gene expression in old workers (Supplemental Fig. S1B,C).

Because hsalHSF2 lacks several functional domains for gene activation found in mammalian hsalHSF2 (see above), we examined whether hsalHSF2 may act in part by cobinding with hsalHSF1 in the absence of heat stress, as observed in mammals (Sandqvist et al. 2009). While the overall correlation between hsalHSF1 and hsalHSF2 binding levels was weak without heat stress in either tissue,

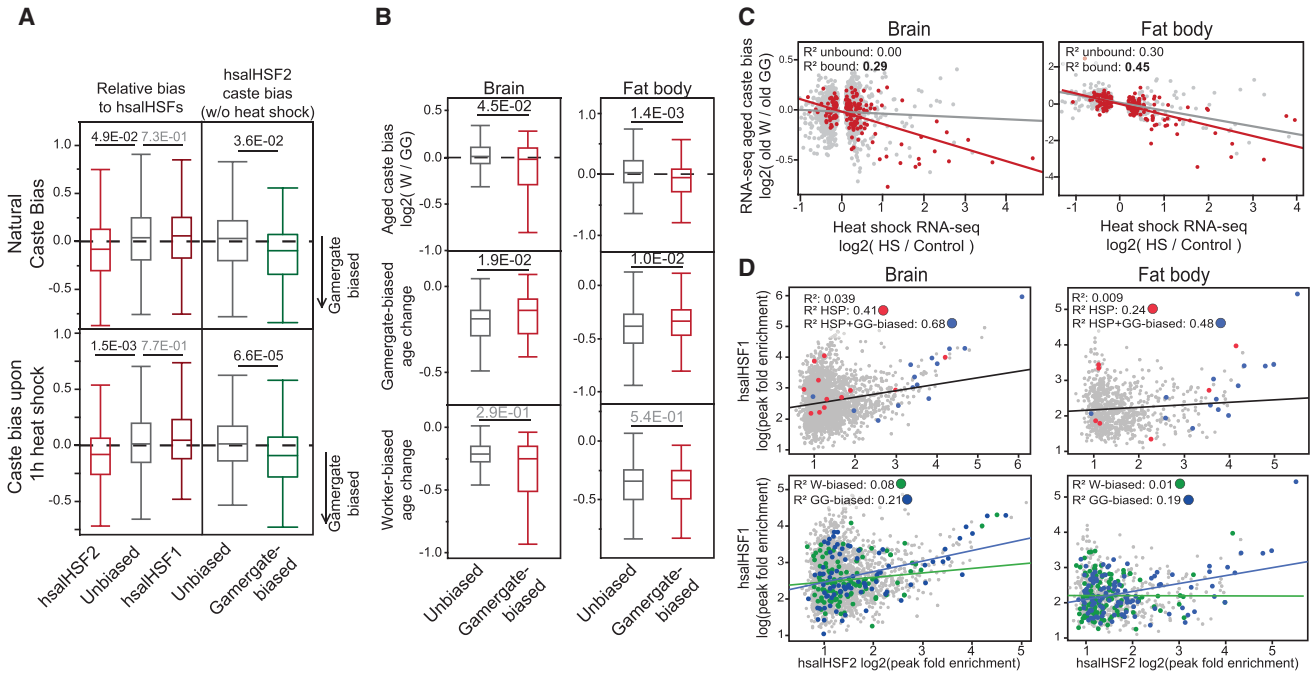

Figure 3. hsalHSF2 in gamergates without heat shock is associated with gamergate bias in old castes. (*A*) For fat body, genes showing higher relative levels of hsalHSF2 binding (as compared with hsalHSF1; *left* plots) as well as genes bound by hsalHSF2 in gamergates without heat shock (*right* plots) show significant bias in gene expression to gamergates in the absence of heat shock (*top*), as well as gene expression bias to heat-shocked gamergates relative to heat-shocked workers (*bottom*). *P*-values are from a Mann–Whitney *U*-test comparing genes with no difference between hsalHSF2 and hsalHSF1 with the respective categories (*left*) or comparing genes with hsalHSF2 bound in gamergates without heat shock with those bound in both castes upon heat shock (*right*). (*B*) Genes bound by hsalHSF2 in gamergates without heat shock that also show a consistent pattern of decreased expression with age irrespective of caste show consistent bias to gamergates (*top*) and higher expression in aged gamergates (*middle*) but lower expression in aged workers (*bottom*) for both brain (*left*) and fat body (*right*) data. *P*-values represent results from a Mann–Whitney *U*-test comparing genes bound by hsalHSF2 in gamergates without HS with genes bound by hsalHSF2 only with heat shock. (*C*) Correlation scatter plots comparing RNA-seq expression bias between heat-shocked and control ants (irrespective of caste) with RNA-seq expression bias between aged castes, divided into genes with (red) and without (gray) hsalHSF2 binding in non-heat-shocked gamergates, illustrating that in both tissues (brain [*top*] and fat body [*bottom*]), basal hsalHSF2 binding in gamergates is associated with genes that show a stronger relationship between heat shock induction and non-heat-shock gamergate bias. (*D*) Correlation scatter plots comparing gene-linked peak enrichment for control hsalHSF2 (*X*-axis) and control hsalHSF1 (*Y*-axis) in brain (*left*) and fat body (*right*) subsets with genes with known chaperone function (*top* row; from Fig. 1F; Supplemental Fig. S2) that are (blue) and are not (red) gamergate-biased, as well as comparing genes showing non-heat-shock caste bias with workers (green) or gamergates (blue) (*bottom*), illustrating that among core HSPs as well as genes biased to gamergates, hsalHSF1 and hsalHSF2 levels show a positive correlation with one another, but outside of these gene categories, there is little relationship.

the cobinding was stronger among chaperone genes, with the strongest relationship for chaperone genes that show gamergate bias (Fig. 3D, top). Furthermore, genes generally biased in expression to gamergates (independent of chaperone function) showed a stronger correlation between basal levels of hsalHSF2 and hsalHSF1 binding than worker-biased genes (Fig. 3D, bottom). This suggests that among heat stress-responsive genes, hsalHSF2 may mediate increased hsalHSF1 binding, and that this relationship may also exist among a subset of gamergate-biased genes.

Overall, these data are consistent with hsalHSF2 in old ants serving to bias expression of a subset of stress response genes to gamergates even in the absence of heat stress, which may in turn explain the stronger differential transcriptional response to heat stress among workers compared with gamergates. Returning to the 17 core chaperone genes biased to gamergates in the fat body, we found that 10 out of 17 of these showed significantly higher worker up-regulation in the fat body with heat stress (as compared with gamergates) (Supplemental Figs. S1C, S8); indeed, inspection of expression level of these genes upon heat stress revealed that this was not due to higher overall worker expression with heat stress, but that the magnitude of up-regulation in workers was higher, and this was largely due to elevated basal expression in unstressed gamergates (Supplemental Fig. S8).

Ectopic expression of HSFs extends fly survival under heat shock and stressed aging

To explore how hsalHSF2 might buffer *H. saltator* gamergates against heat stress and extend life span, we expressed ant hsalHSF1 and hsalHSF2 in *D. melanogaster*. We produced fly lines with UAS-driven ectopic expression of hsalHSF1 and hsalHSF2. As controls, we generated flies

expressing the *D. melanogaster Hsf* gene or nuclear RFP from the same fly background, driver, and reporter construct as those used for hsalHSFs (see Supplemental Fig. S9A for validation). We crossed these flies with elav-Gal4 and PPL-Gal4 driver lines to produce flies expressing these genes in neurons and fat body cells, respectively.

We evaluated survival under heat stress of varying intensities: 45 min at 41°C, 4 h at 37°C, and 24 h at 35.5°C. For most conditions, strikingly, hsalHSF2 ectopic expression led to increased survival under heat stress conditions compared with our nRFP overexpression control (Fig. 4A, B; Supplemental Tables S9, S10). Furthermore, despite much higher similarity of hsalHSF1 to fly dmHSF, hsalHSF1 showed less buffering against heat stress compared with hsalHSF2. When expressed in neurons, hsalHSF1 did not significantly differ from nRFP ectopic expression controls, except in the context of 24-h heat stress (Fig. 4A, right), while, in the fat body, all three HSF ectopic lines showed increased survival relative to the nRFP control (Fig. 4B).

We performed a short-term mild stress-associated "aging" assay at 30°C, simulating longer-term low-stress conditions (Morrow et al. 2004). As with the stronger heat stress (Fig. 4A,B), ectopic expression of HSFs led to longer life span, with dmHSF and hsalHSF1 showing intermediate life span extension (median life span: dmHsf elav: 29 d, PPL: 30 d; hsalHSF1 elav: 27 d, PPL: 34 d) (Fig. 4C; Supplemental Tables S11, S12). Strikingly, again, hsalHSF2 overexpression led to improved survival compared with our control overexpression line, showing >50% higher median life span in this context relative to nRFP controls (hsalHSF2 median elav: 36 d, PPL: 38 d) (Fig. 4C; Supplemental Tables S11, S12).

Additionally, we observed increased locomotor activity in our hsalHSF2 ectopic expression flies and performed a common assay to assess fly age-associated locomotion decline (climbing assay) (see the Materials and Methods) at d19 and d21 (for elav- and PPL-driven expression, respectively). The hsalHSF2-expressing flies outperformed all other lines in climbing after ~20 d under mild heat stress (Fig. 4D; Supplemental Table S9). This was particularly striking for PPL-driven fat body expression, despite the nonneuronal expression of hsalHSF2 (Fig. 4D, right).

Importantly, in a conventional aging assay, we observed that flies expressing hsalHSF2 showed a 30% extension of life span (hsalHSF2 life span: 87 d, both drivers) (Fig. 4E; Supplemental Fig. S9B; Supplemental Table S11). Thus, remarkably, compared with hsalHSF1 or *dm*HSF, hsalHSF2 extension of life span operates beyond buffering against heat stress (Fig. 4C) and also plays a role in extending life span (Fig. 4E), suggesting the same mechanism may be operating in *H. saltator*.

Conserved targets mediate stress-buffering and life span extension of hsHSF2 in ant flies

We explored the mechanism whereby hsalHSF2 expression in flies increases survival under stressed and aging nonstressed conditions, performing RNA-seq of the four ectopic fly lines (hsalHSF1, hsalHSF2, hsalHsf, and nRFP) driven in the fat body (PPL) with and without heat shock. Consistent with longer survival, the hsalHSF2 flies showed a distinct transcriptional signature with and without heat stress (Fig. 5A). We compared each distinct fly line with all others for both control and heat stress conditions, finding that the number of genes differentially expressed between hsalHSF2 flies compared with all others was remarkably higher than for any other fly line (Fig. 5A). Examination of functional enrichment of genes more highly expressed in hsalHSF2 flies in control without heat stress revealed strong enrichment of functional terms related to protein folding and chaperone activity (Fig. 5A, top right, red; Supplemental Table S13). Genes more highly expressed in heat-stressed hsalHSF2 flies showed enrichment for mitochondria-related functions, chromatin modification, and DNA repair terms (Fig. 5A, bottom right; Supplemental Table S13).

This transcriptional difference between hsalHSF2 flies and the other flies was underscored by PCA of our fly RNA-seq samples (see the Materials and Methods) showing strong differentiation of hsalHSF2 flies relative to all others, regardless of heat stress (Fig. 5B). Despite the observation that dmHSF and, in some contexts, hsalHSF1 ectopic flies showed moderately enhanced survival (Fig. 4B,C), in stark contrast to hsalHSF2, they did not differ substantially in transcription from one another or from nRFP flies with or without heat stress (Fig. 5A,B).

Given this and our results from *H. saltator*, we examined individual genes contributing to the enrichment of chaperone-related functions among basal non-heat-stressed hsalHSF2 flies. Of the 222 genes more highly expressed among non-heat-stressed hsalHSF2 flies, 17 were directly annotated with the term "protein folding" and 30 were directly annotated with the term "response to stress." We compared across species to discover conserved genes activated by ant hsalHSF2 that might regulate heat resilience and life span. Over half of the genes annotated with "protein folding" (nine out of 17) were also significantly more highly exressed in at least one tissue in gamergates and/or up-regulated preferentially as gamergates age (seven in the fat body and six in brains) (Fig. 5C; Supplemental Fig. S9C; Supplemental Table S14).

We investigated whether ectopic hsalHSF2 expression led to this remarkably strong distinct transcription via binding of target genes without heat stress using ChIP-seq of hsalHSF1 and hsalHSF2 in the fat body (PPL) ectopic expression flies. Of the 17 chaperone genes more highly expressed in control hsalHSF2 flies versus others, we found that 11 featured an hsalHSF2 peak in non-heat-shocked samples (four shown in Fig. 5D; Supplemental Tables S14, S15), similar to our ant results. Of the nine genes showing hsalHSF2 fly expression bias and also gamergate expression bias, eight featured an hsalHSF2 peak in flies and all featured an hsalHSF2 peak in gamergates without heat shock, implying that many are directly up-regulated by hsalHSF2 binding and that this mechanism similarly occurs in gamergates.

For both hsalHSF1 and hsalHSF2, binding was observed with and without heat stress, with hsalHSF1 showing many more bound loci than hsalHSF2 (Supplemental Fig.

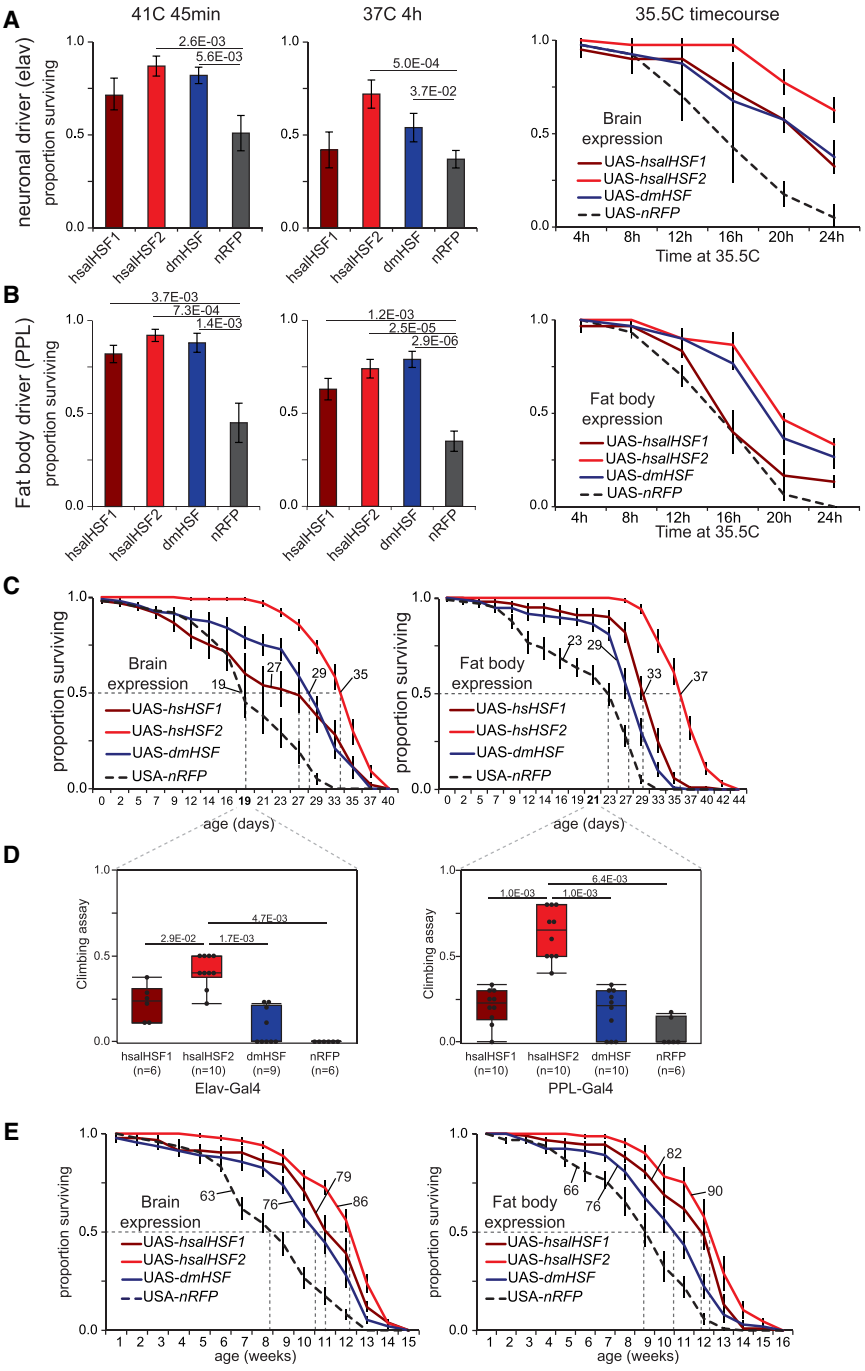

Figure 4. Ectopic expression of HSFs increases survival with heat shock and extends fly life span. (*A*) Proportion of flies ectopically expressing *H. saltator* HSF1, *H. saltator* HSF2, *D. melanogaster Hsf*, or nRFP (identical genetic background) in neurons that survived short-term high heat (45 min at 41°C; *left* plot; $n = 10$ vials of 10 flies each), medium heat stress (6 h at 37°C; *middle* plot; $n = 10$ vials of 10 flies each), and 4-h time points across a survival time course under mild heat stress (35.5°C; *right* plot; $n = 3$–4 vials of 10 flies per time point). *P*-values represent results from a Kruskal–Wallis test followed by a Dunn's test for all pairwise comparisons between nRFP overexpression flies and each HSF overexpression fly line. (*B*) The same as in *A* but for fat body-driven ectopic expression of the same genes. (*C*) Life span assay of flies ectopically expressing *H. saltator* HSF genes, *D. melanogaster Hsf*, or ornRFP (identical genetic background) when kept at 30°C. (*Left*) Neuronal ectopic expression driven under elav. (*Right*) Fat body ectopic expression driven under PPL. Numbers labeling lines represent median life spans for given curves. $n = 10$ vials of 10 flies per line. (*D*) Results of climbing assay taken from the indicated day of 30°C aging assay. *P*-values represent results from a Kruskal–Wallis test followed by a Dunn's test for all pairs comparing hsalHSF2 flies with transgenic fly lines. (*E*) Results from life span assay performed at 25°C for ectopic HSF expression lines (or nRFP-negative control; $n = 10$ vials of 10 flies each) for driven neurons (*left*; elav) or fat body (*right*; PPL). Numbers labeling lines represent median life span for the given curve.

S10A,B), similar to our obervations in *H. saltator* (Supplemental Figs. S4D, S5B). Also similar to *H. saltator*, despite the abundance of hsalHSF1 binding in flies, hsalHSF1 binding was less predictive of heat stress gene up-regulation than hsalHSF2 binding (Supplemental Fig. S8C). hsalHSF1 also showed a lower increase in binding upon heat stress relative to hsalHSF2 (Supplemental Fig. S10D). For hsalHSF2, this may reflect a natural propensity to bind in an expression level-dependent manner (in contrast to HSF1) (Åkerfelt et al. 2010), whereby increased expression of hsalHSF2 leads to increased binding and up-regulation of target genes, as in ants. In contrast, for hsalHSF1, this may be due to either ectopic expression, leading to excess hsalHSF1, or protein divergence between hsalHSF1 and dmHSF, leading to an inability of hsp90 to bind to hsalHSF1 in nonstressed conditions to retain hsalHSF1 in the cytoplasm, as typical for HSF1/*Hsf*. This is supported by the fact that in ants, hsalHSF1 binds far fewer genes in the fat body without heat stress than with heat stress (Supplemental Fig. S5C, bottom right plot). We note an important control for the hsalHSF2 fly ChIP-seq: ChIP-seq of hsalHSF2 in hsalHSF1 flies ensures

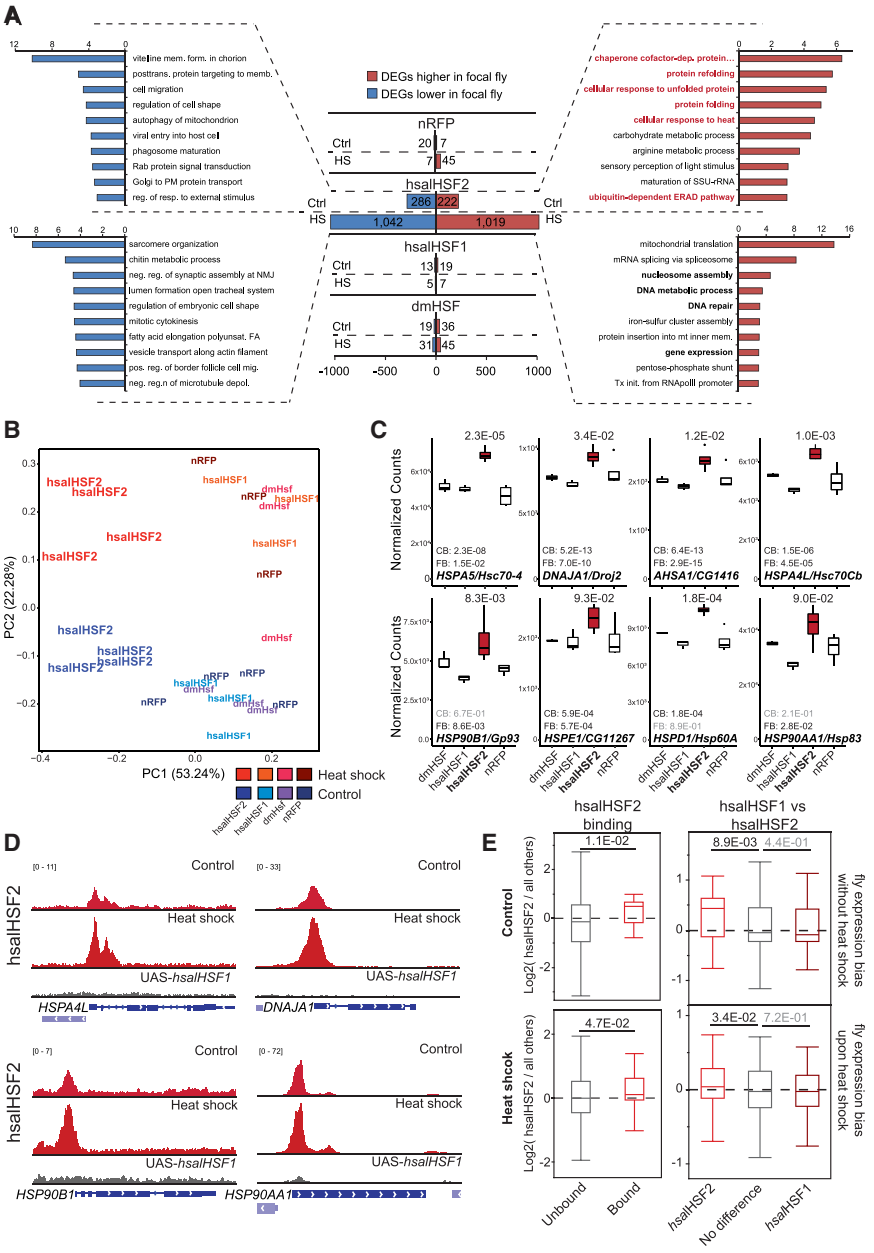

Figure 5. Genome-wide characterization of HSF ectopic expression flies reveals conserved targets and binding with ants. (*A*) Numbers of differentially expressed genes between the given ectopic fly line and all others here for heat-shocked samples (*top* bars of each pair) and non-heat-shocked samples (*bottom* bars for each pair), illustrating strong departure of hsalHSF2 flies from others shown. The offset bar plots represent the top 10 significant gene ontology terms (Biological process) enriched among the respective groups of hsalHSF2 up-regulated or down-regulated genes. Terms in red illustrate the strong presence of genes with functions related to managing misfolded proteins among hsalHSF2 flies in the absence of heat shock, similar to what is seen in natural gamergates. (*B*) Principle component analysis of RNA-seq from all transgenic fly samples, illustrating the transcriptionally distinct nature of hsalHSF2-overexpressing flies relative to all others. PCA generated using VST transformed counts of all genes differing significantly ($P\text{adj} < 0.01$) in a combined model modeling genetic line and heat shock status. (*C*) Normalized count plots of non-heat-shocked fly samples illustrating key chaperone genes most highly expressed in hsalHSF2 flies without heat shock that also feature significant gamergate bias in *H. saltator* aging RNA-seq. For RNA-seq, $n = 3$–4. *P*-values shown at the *top* of each plot represent the significance of comparing hsalHSF2 samples with other lines (DESeq2 adjusted *P*-values). *P*-values shown *above* gene names represent adjusted *P*-values taken from *H. saltator* caste comparisons between old gamergates and workers, reflecting the significance of *H. saltator* gamergate bias in each tissue. (CB) Central brain adjusted *P*-values, (FB) fat body adjusted *P*-values. (*D*) Example genome browser tracks from four genes featuring hsalHSF2 heightened expression without heat shock as well as hsalHSF2 binding in the same context. Show *below* the heat shock and control tracks are tracks from ChIP-seq using the antibody targeting hsalHSF2 in heat-shocked hsalHSF1 flies. Tracks represent reads per million (RPM) averaged across replicates ($n = 2$). (*E*) Box plots of average $\log_2$ expression ratios for DEGs between hsalHSF2 flies and all other fly lines analyzed here, illustrating that hsalHSF2 binding (as determined by peak presence in ChIP-seq of transgenic flies) is predictive of hsalHSF2 fly transcriptional bias (*left*), as is higher relative enrichment of hsalHSF2 (vs. hsalHSF1) (*right*) for both flies in the absence of heat shock (*top*) and heat-shocked samples (*bottom*). *P*-values from a Mann–Whitney *U*-test comparing genes without hsalHSF2 or with no difference between hsalHSF2 and hsalHSF1 with the respective categories.

hsalHSF2 antibody specificity, yielding little apparent cross-reactivity with hsalHSF1 (or endogenous dmHSF) (Fig. 5D, gray tracks; Supplemental Fig. S10A).

Finally, we found that hsalHSF2 binding was broadly predictive of expression bias in flies (Fig. 5E, left; Supplemental Fig. S10E, bottom left), supporting the hypothesis that specific hsalHSF2 binding led to increased hsalHSF2 fly life span and stress resistence. In contrast, hsalHSF1 binding was poorly predictive of fly-biased expression (Fig. 5E, right; Supplemental Fig. S10E, left top) despite these flies showing survival differences from controls in some heat shock and aging experiments (Fig. 4; Supplemental Fig. S9B); this poor correlation may be due to the few DEGs biased to hsalHSF1 flies (Supplemental Table S14). We perfomed the same comparison of ChIP-seq binding with RNA-seq using the hsalHSF2 line relative to nRFP control flies, yielding highly similar results (Supplemental Fig. S10F). We also compared DEGs in hsalHSF2 flies also

bound by hsalHSF2 with *H. saltator* RNA-seq. Here, for both brains and the fat body, ant orthologs of fly genes that were more highly expressed in hsalHSF2 flies showed gamergate bias among old ants (Supplemental Fig. S10G, top) and also exhibited an age-related decrease in expression for workers but not gamergates (Supplemental Fig. S10G, bottom).

Taken together, we found that hsalHSF2 binds to and up-regulates chaperone genes in control nonstress conditions in both *H. saltator* and *D. melanogaster*; these genes likely contribute to increased heat stress resilience as well as extended life span of both *H. saltator* gamergates and hsalHSF2 flies (Fig. 6).

Discussion

The remarkable differential life spans of the reproductive caste compared with the worker caste in ant societies provide an unparalleled experimental model for uncovering mechanisms underlying aging in complex organisms. The heat shock response pathway has long been investigated for transcriptional control of proteomic surveillance in both heat stress and aging. Our results show that HSR pathway genes that are generally up-regulated upon heat stress (in both castes) are strongly gamergate-biased in expression in basal nonstress conditions and also either are increased in expression with gamergate aging or are decreased in workers while maintained in gamergates. The key mechanistic finding of our study that may explain the differential gene expression is that *H. saltator* encodes a gene with apparent homology with mammalian HSF2 (as do all Hymenoptera examined) (Supplemental Fig. S2C), and that *hsalHSF2* specifically is increased in expression as gamergates age but is decreased or remains lowly expressed in workers (Fig. 2A). Genome-wide profiling of hsalHSF2 and hsalHSF1 shows distinct binding patterns (Fig. 2; Supplemental Fig. S6B), and—perhaps critically—exclusively in gamergates, hsalHSF2 is bound to DNA even under basal conditions (Fig. 2D; Supplemental Figs. S2E, S6A,B); this binding corresponds to gamergate-biased gene expression of multiple core chaperone proteins crucial to proteostasis (Fig. 1C; Supplemental Fig. S1B,S1C).

A second illuminating finding of our study is that transgenic expression of hsalHSF2 in flies led to improved survival under multiple heat stress regimes and to extension of fly life span without heat stress; this resilience was greater than observed for flies overexpressing hsalHSF1 or dmHSF (Fig. 4). Profiling of the fly transcriptomes and fly hsalHSF2 binding revealed conserved, distinguishing features common between transgenic flies and *H. saltator* gamergates (Fig. 5C,D; Supplemental Figs. S9, S10A,B), underscoring the importance of hsalHSF2 in accomplishing life span extension in gamergates. These findings have far-reaching implications due to the widely conserved link between the negative consequences of aging and breakdown of proteostasis.

The remarkable life span disparity between reproductive and worker social insect castes may result from reduced mortality among nest-bound reproductive ants (as worker ants are subject to environmental stresses). This removes evolutionary pressures that typically encourage investment in early-life reproduction at the cost of life span but maintains the fundamental benefit of a longer reproductive life (and thereby produces more direct offspring) (Jemielity et al. 2005). Because of this, the worker/reproductive longevity divergence in social insects provides an outstanding example of natural selection of epigenetic life span regulation (Kozeretska et al. 2017). *H. saltator* in particular represents an exceptional model for studying this phenomenon because any worker in the colony can transition to reproductive status (called gamergate) accompanied by a fivefold increase in life span (Fig. 1A). In this study, we discovered that, along with life span extension, gamergates are buffered against heat stress-induced mortality, while workers suffer the common decrease in heat stress survival with age (Fig. 1D; Supplemental Fig. S1D; Taylor and Dillin 2011). Thus, the gain in heat stress survival is specific to the *H. saltator* gamergate state, as is life span of >3 yr. This is in contrast to workers, who show a greater susceptibility to heat stress and a life span of only ~6–8 mo. Our study reveals that (1) gamergates exhibit a strong, global transcriptomic signature of up-regulating HSR genes (chaperones and stress resposnse genes) under basal conditions and with increased age; (2) in addition to the common HSF1 homolog, the *H. saltator* genome (as

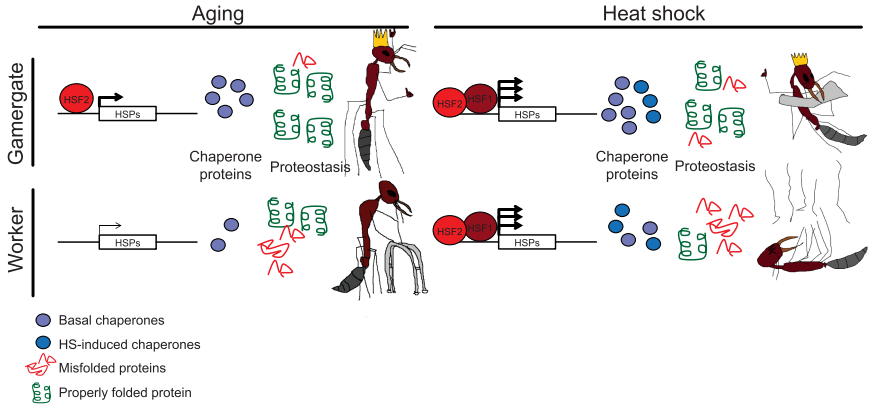

Figure 6. Model of hsalHSF2-mediated proteostasis in gamergates. (*Left*) Under normal conditions, hsalHSF2 preferentially binds and up-regulates chaperone genes in gamergates, leading to eleveated (or maintained, age-invariant) levels of chaperone proteins, maintaining proteostasis with increased age, while workers experience the commonly observed loss of proteostais with age. (*Right*) Upon heat stress, higher basal levels of chaperone proteins in gamergates complement the caste-invariant heat shock response, leading to better management of heat-induced protein misfolding and increased survival of gamergates during heat stress.

well as those of many other insects) encodes an *HSF2*-like gene that is considerably elevated in gamergates with increased age (but declines in workers with age); (3) hsalHSF2 shows a striking gamergate specificity in binding under basal (non-heat-stress) conditions, and this binding is predictive of up-regulation of stress response genes; and (4) transgenic expression of hsalHSF2 in flies provides resistance to heat stress, extends life span, and up-regulates chaperone genes. These findings strongly implicate hsalHSF2 in a key role to activate a cohort of protective genes (discussed in below) that confer resistance to heat stress and long life span.

Studies in model systems strongly link proteome "health" with longevity because protein misfolding increases with age in many models (Soti and Csermely 2003; Calderwood et al. 2009; Dukay et al. 2019), coincident with decreasing efficacy of the HSR (Calderwood et al. 2009; Liang et al. 2014). In the short-lived worker ants, we observed considerably lower survival following heat stress than in the long-lived gamergates, and this pattern becomes more pronounced in older ants (Fig. 1D; Supplemental Fig. S1D), suggesting that gamergates effectively manage negative consequences of protein misfolding compared with workers. This could be due to either a more rapid and elevated HSR upon heat insult or an overall "healthier" proteome in gamergates that buffers against rapid heat-induced proteomic stress. Consistent with the latter hypothesis, we observed expression of multiple chaperone proteins that were naturally biased to gamergates in RNA-seq data taken from two tissues of young and old ants (Fig. 1C; Supplemental Fig. S1B,C). More generally, genes differentially regulated by heat stress in *H. saltator* correlated with genes showing gamergate-biased expression during aging in natural samples due to either increased gamergate expression or decreased worker expression with age (Fig. 1E,F; Supplemental Figs. S1A, S4A). Overall, these findings indicate that, at the basal level, gamergates use genes typically differentially expressed upon heat stress to repurpose them during aging. This also explains our findings that gamergates show fewer DEGs with heat stress—specifically that gamergates show basal elevated expression of these genes in non-heat-stress conditions, and indeed, many of these genes reach a similarly high level of expression upon heat stress, matching levels in workers (Fig. 3E; Supplemental Fig. S1B,S1C). This is similar to what has been observed in *D. melanogaster*, whereby mild heat shock, resulting in production of HSPs, considerably increases survival when followed by a severe heat shock (Mitchell et al. 1979).

In mammals, HSF2 is distinct from HSF1 in its activity and binding specificity (Åkerfelt et al. 2010). While *H. saltator*'s "HSF2" is distinct from mammalian HSF2 in that it lacks several C-terminal domains present in both human HSF1 and HSF2, hsalHSF2 shows closer sequence homology with human HSF2 in the remaining protein compared with HSF1 or HSF4 (Fig. 2B). In addition, our finding that hsalHSF2 binds without heat shock primarily in the gamergate genome is consistent with findings in mammals related to non-heat-stress HSF2 binding with concurrent gene up-regulation (Sandqvist et al. 2009). Furthermore, *hsalHSF2* shows the highest expression in early stage (<4 d) *H. saltator* eggs (developing embryos) (Supplemental Fig. S5A, left), consistent with what has been seen in vertebrate models (Mezger et al. 1994; Kawazoe et al. 1999; Choi et al. 2011). Given *hsal*HSF2's conservation among many noneusocial insects (Supplemental Fig. S4C), the ancestral function of *hsal*HSF2 may be developmental, and its function in *H. saltator* gamergates is an exaptation of this conserved role. While mammalian HSF2 has not been linked to life span extension, loss of HSF2 is associated with stress-associated loss of proteostasis (Shinkawa et al. 2011).

Currently, the mechanistic basis of *hsal*HSF2 binding and gene activation is unclear. In mammals, HSF2 forms heterotrimers with HSF1, while we detected only limited HSF1 binding without heat stress at *hsal*HSF2 binding sites (mostly in the brain); we speculate that heterotrimerization may occur upon heat stress and HSF1 disassociation from Hsp90 to bind to *hsal*HSF2 (Fig. 2B). However, conservation of the oligomerization domain in *hsal*HSF2 is limited (Fig. 2B). In addition, *hsal*HSF1 binding is less predictive of gene up-regulation upon heat stress compared with *hsal*HSF2; this weaker association may be due to *hsal*HSF1 binding many genes that are not up-regulated during heat stress, rather than a lack of targeting to heat stress up-regulated genes.

Supporting a specific role of *hsal*HSF2 in mediating enhanced response to heat stress and general aging in gamergates, ectopic expression of *hsal*HSF2 in *D. melanogaster* led to notable increases in fly survival following multiple heat shock regimes (Fig. 4A–C), including aging under mild heat (30°C) and aging in the absence of heat (Fig. 4E). Ectopic expression of *hsal*HSF1 and dmHSF provided increased survival but to a lesser extent, suggesting that overexpression of HSFs in general increases robustness in response to heat stress and general life-long proteomic insult, as seen in *C. elegans* (Hsu et al. 2003; Morley and Morimoto 2004); however, binding of HSF1/dmHSF by HSPs may dampen the impact of ectopic expression of these versus *hsal*HSF2. Transcriptome sequencing of the ectopic fly lines revealed a strong distinction between *hsal*HSF2 flies and the other HSF ectopic flies (and nRFP controls) for both non-heat-stressed and heat-stressed flies (Fig. 4). Remarkably, multiple genes elevated in basal gamergates and bound by *hsal*HSF2 in *H. saltator* showed a strikingly similar pattern of up-regulation in control *hsal*HSF2 ectopic flies; indeed, among the 222 genes biased to *hsal*HSF2 flies without heat stress were multiple enriched functional terms related to protein folding and chaperone activity (Fig. 5A). Furthermore, gene terms showing a similar pattern of *hsal*HSF2 fly bias with heat stress were enriched for DNA repair and gene expression regulation, suggesting that upon heat stress, *hsal*HSF2 also causes distinct changes in gene expression that may contribute to enhanced surivival of gamergates upon heat stress.

Genome-wide profiling of *hsal*HSF1 and *hsal*HSF2 in ectopic fly lines revealed a contrast similar to that in gamergates: *hsal*HSF1 was more broadly bound, while *hsal*HSF2 bound fewer genes, but the binding was,

amazingly, more predictive of heat stress up-regulation than *hsal*HSF1 (Supplemental Fig. S10C). *hsal*HSF2 binding was also more predictive of *hsal*HSF2 fly-biased expression both with and without heat stress (Fig. 5E; Supplemental Fig. S10E), whereas *hsal*HSF1 flies showed far fewer genes showing *hsal*HSF1-specific expression with or without heat stress (Fig. 5A). Precisely how this is achieved at the molecular level given the absence of a TAD in *hsal*HSF2 is an important question; nonetheless, we propose that our consistent results in flies validate our findings in *H. saltator*, showing that *hsal*HSF2 induces chaperone gene expression and does so in a stress- and age-protective manner. Furthermore, remaining to be answered is why only a subset of genes bound by *hsal*HSF2 in non-heat-shock conditions (in either species) shows up-regulation; however, it is likely that other mechanisms and transcription factors are at play to mediate the preferential up-regulation of only certain genes bound by *hsal*HSF2.

Recent findings show that one mechanism in *H. saltator* potentially mediating association between reproductive status and extended life span is blocking of AKT phosphorylation in gamergate fat body, despite the elevated insulin signaling associated with ovary activation (Yan et al. 2022). This leads to gamergate-specific increased nuclear localization of the transcription factor FOXO, and increased nuclear FOXO activity has associated with increased life span in *D. melanogaster*, *Caenorhabditis elegans*, and *Mus musculus* (Martins et al. 2016). Because perturbations of the insulin pathway in models never reach the level of life span extension in *H. saltator* gamergates, other mechanisms contribute to extended life span of reproductive ants. Interestingly, HSF1 is regulated by insulin (Barna et al. 2012) and is necessary for life span extension associated with insulin signaling defect mutants in *C. elegans*, which is due, in part, to FOXO requiring HSF1 to activate some downstream gene targets (Hsu et al. 2003). Hence, *hsal*HSF2 may act similarly and downstream from the altered insulin documentented in reproductive ants (Yan et al. 2022).

*hsal*HSF2 is unlikely to be the only factor mediating the extreme life span extension seen in gamergates and may be specialized to mitigate proteomic stress associated with long life span in gamergates compared with workers. While in most ants the queens are much longer-lived (relative to the workers in the same species) compared with *H. saltator* gamergates (Keller 1998), queens in these other ants are typically developmentally fixed, showing very strong, permanent changes to physiology. In *H. saltator*, in contrast, any worker can transition to gamergate during adulthood. Instead, in the transition to gamergate, normally short-lived workers extend life span up to fivefold, relying on postdevelopmental mechanisms. These may include conditionally induced genes to mediate the molecular component of extended life span, such as up-regulation of HSFs to increase chaperone levels facultatively to combat age-associated proteome insult. However, this is only one negative consequence of aging, and hence other mechanisms will be invoked to manage other age-related degenerative factors such as transcription and epigenome regulatory instability, oxidative damage (Schneider et al. 2011), genome integrity, and neuronal decline (Sheng et al. 2020).

One question related to this is why *hsal*HSF2 is so strikingly up-regulated in old gamergates (Fig. 2A) while many chaperone proteins bound by *hsal*HSF2 in the absence of heat stress in old gamergates show expression bias to old gamergates due at least in part to a decline in worker expression with age (either with or without increased gamergate expression with age). It is possible that a major function of *hsal*HSF2 is to maintain (rather than increase) HSP gene expression as gamergates age, which would otherwise decline, as in workers (Fig. 1B; Supplemental Fig. S1B,C). In this case, other mechanisms that decline with age promote expression of these genes in young ants, while *hsal*HSF2 up-regulation serves as a caste-specific mechanism to maintain their expression in old gamergates. A related question is whether *hsal*HSF2 prevents proteostatic decline in aging gamergates or rather is a gamergate-specific mechanism to mitigate increased proteomic decline in long-lived gamergates. Either effect represents a gamergate-specific mechanism (consistent with our data); however, prevention would represent a gamergate-specific step upstream of aging changes, whereas mitigation represents a gamergate-specific response to aging-associated decline.

Another general issue is, in a system where adult plasticity can accomplish such considerable life span extension "on command," why not all individuals within a colony use these mechanisms. One explanation is that these are costly or confer an unseen disadvantage to workers (Krebs and Loeschcke 1994). Alternatively, extending nonreproductive life span may provide little benefit to natural colonies due to worker mortality associated with extrinsic risk in the wild (Kramer and Schaible 2013a), with an added energenic cost of higher colony investment in longer-lived workers (Kramer and Schaible 2013b). Nonetheless, the striking plasticity of life span in eusocial insects provides an outstanding study system, and given the deep conservation in proteostasis in aging, the new major component of differential longevity conferred by *hsal*HSF2 may reveal broad biological implications.

Materials and methods

H. saltator *ants*

All *H. saltator* used in this study originated as described in Gospocic et al. (2017). The genetic background origin of each sample was recorded (Supplemental Table S16), balanced (treatment and control from the same colonies), and used in RNA-seq statistical testing as a blocking variable.

H. saltator colonies were housed in plastic boxes with a plaster nest chamber in a temperature-controlled (25°C) and humidity-controlled (50%) ant facility on a 12-h light/dark cycle. Ants were fed three times per week with live crickets, and plaster was wet with water to prevent desiccation of the ant brood.

For ant survivorship curves (Fig. 1A), 48 *H. salataor* colonies were established by isolation of 30 age-matched newly eclosed workers. Founding workers were paint-marked with two colors in such a way that no worker from a given transition shared a paint code with another from the same transition. Dueling was scored for at least 5 d starting from d2 of isolation (peak dueling)

(Gospocic et al. 2017) in order to identify resulting gamergates. After ≥210 d, all painted ants (founding workers/gamergates) were compared with dueling records, and any designate gamergates (dueling more than three out of five observations) were wire-tagged with thin colored wire (34-gauge colored beading wire; Artistic Wire) by tying a small loop at the petiole in order to permanently identify these ants. Following this, every week, all new callows in each of these colonies were painted with a distinct two-color paint combination each week using two colors selected from among 13 distinctly colored paints (Testors acrylic paints). This resulted in >160 potential color pair combinations (13^2), resulting in no color pair repeating for >3 yr. For each colony, the number of painted callows was recorded each week. After 9 mo of such weekly paintings, censuses were performed on all colonies, comparing number of observed workers with a given paint combination versus recorded number of initially painted callows. This was repeated twice (total of three batches), spaced at least 2 mo apart (Supplemental Table S1). Only worker cohorts with an initial number of painted workers ≥10 were used for Figure 1A, and each batch consisted of six to 10 censused colonies, for a total n per time point of 25–30 (Supplemental Table S1).

For gamergate assessments, founding gamergates featuring wire tags were assessed across these colonies periodically. Only colonies with four or more initial wire-tagged gamergates were used, and assessments were done in six batches performed periodically across 24 mo. For each batch (Supplemental Table S1), up to five colonies with four or more founding gamergates were assessed based on the gamergate age falling within 2 wk of each 10-wk-separated time point, resulting in each time point being represented by $n = 25–30$. All numbers related to gamergate and worker life span assessments are shown in Supplemental Table S1.

For RT-qPCR assessment of *hsalHSF2* expression (Supplemental Fig. S5A), two established colonies (<100 ants; d180 and d175) were used. L1 and L4 larvae were collected based on gross morphology. For pupae, white pupae with colored eyes (~15 d as pupae) were collected, and the brains were dissected. For pupal fat body, due to the disassociation of fat body cells during pupal development, pupa were first punctured, and suspected fat body cells were extracted by gently squeezing the pupa in a 100-µL drop of HBSS that was saved for RNA extraction, followed by dissection of the brains in a second drop. For eggs, all eggs were first removed from the two colonies. After 3 d, four new eggs were collected for each early egg time point sample ($n = 4$ for all RT-qPCR samples, twice from each colony). This was repeated, but eggs were instead transferred to a nest with workers, where they were kept for 15 d to ensure all eggs were >15 d old. For adult tissues, age-matched gamergates and workers were collected from the same colonies. For ovary dissections, only germarium were used to avoid inclusion of more mature oocytes in the samples.

For heat shock survival assessment (Fig. 1D), transitions of age-matched gamergates and workers of given ages (Supplemental Table S4) were incubated for 18 h at 36.5°C in nest containers containing moistened plaster. Following this, ants were removed from the incubator and allowed to recover for 1 h, and reproductive status was assessed for all living and deceased ants. Only transition colonies containing eight or more original individuals were used.

D. melanogaster

All flies were raised at 25°C and 50% humidity on a 12-h light/dark cycle using standard Bloomington *Drosophila* medium (Nutri-Fly). The PPL-Gal4 driver (58768) and elav-Gal4 driver (8760) lines were purchased from the Bloomington *Drosophila* Stock Center. The UAS-hsHSF1, UAS-hsHSF2, and UAS-dmHsf transgenic lines were generated by cloning the *H. saltator* or *D. melanogaster* cDNA for the respective genes into pBID-UASC (Wang et al. 2012), followed by PhiC31 integrase-mediated transgenesis into the attP40 landing site on chromosome 2, performed by BestGene. The UAS-nRFP genetic line was generated as above but using a donor plasmid provided by the Bonasio laboratory for the nRFP insert.

RNA-seq samples, extraction, and library preparation

H. saltator central brains or fat body were dissected from single individuals, snap-frozen, homogenized in TriPure (Sigma), and isolated via precipitation in 2-Propanol.

For the caste aging RNA-seq data set, gamergates were established as described above. Worker samples were taken from stable colonies used in survivorship estimation, featuring painted, age-matched worker cohorts. This was done to minimize the potential that workers would represent reverted gamergates, which is more common in newly established *H. saltator* hierarchies (e.g., dueling colonies used for gamergates). Gamergates and workers of d40 were collected to represent young ants. For old ants, workers aged d220–d235 were used to capture workers near end of life, given that worker mortality greatly increases at ~d240 (Fig. 1A). For old gamergates, a subset ($n = 5$) was collected from the same age range as workers (d220–d235), while another subset was taken from gamergates of ages ≥1 yr.

For the *H. saltator* heat shock RNA-seq experiment, age-matched gamergates and workers aged d215–d224 (Supplemental Table S16) were collected as for aging RNA-seq above immediately prior to heat shock (<1 h), split into two equal-numbered groups of gamergates and workers (with one half placed within a preheated container containing moistened dental plaster), and incubated for 1 h at 39.5°C, followed by recovery for 15 min. Following recovery, samples were immediately anesthetized on ice, and tissues were dissected and snap-frozen in liquid nitrogen. For control samples, individuals from the same age-matched pools were dissected at the same time to ensure matched cohorts.

For RNA-seq, polyadenylated RNA was purified from total RNA using the NEBNext poly(A) mRNA magnetic isolation module (NEB E7490) with on-bead fragmentation as described (Zhong et al. 2011). cDNA libraries were prepared the same day using the NEBNext Ultra II directional RNA library preparation kit for Illumina (NEB E7760). All samples were amplified using eight cycles of PCR.

RT-qPCR

Samples were collected, and RNA was extracted as described above. Thirty-three percent of the resulting isolated total RNA was reverse-transcribed with random hexamers using the high-capacity RNA-to-cDNA kit (Applied Biosystems). cDNA samples were then diluted 1:3, and RT-qPCR was performed on four biological replicates (triplicate technical replicates) for each stage/tissue. Abundance of *hsalHSF2* transcripts was estimated using Power SYBR Green PCR master mix (Life Technologies) on a real-time qPCR machine using the primer sequences *hsalHSF2* forward (AACGGCGATACCATACTGCT), *hsalHSF2* reverse (GCGAAAACTGTCGTGCAGAA), *RPL32* forward (CGTAGGC GATTTAAGGGTCA), and *RPL32* reverse (TTTCGGAAGCCA GTTGGTAG).

Relative transcript abundance was estimated using the $\Delta\Delta Ct$ method (Livak and Schmittgen 2001). For worker/gamergate tissues, pupal brains and fat body as well as early eggs were repeated for this run in order to increase comparability of results between runs.

ChIP sequencing

For ChIP sequencing, samples were collected and heat-shocked as described above for heat shock RNA-seq (Supplemental Table

S16). Only ages with ≥14 samples for each caste were used and split into equal numbers of each caste immediately prior to heat shock.

Following heat shock and recovery, brains and fat body were dissected from seven *H. saltator* ants per ChIP-seq sample on ice. Immunoprecipitation was performed as described by Glastad et al. (2020) and Gospocic et al. (2021).

Libraries for sequencing were prepared using the NEBNext Ultra II DNA library preparation kit for Illumina (NEB E7645) as described by the manufacturer but using half volumes of all reagents and starting material. Thirteen cycles of PCR were used for hsalHSF1 and hsalHSF2 libraries, and six cycles were used for input controls. The first two replicate ChIP-seq experiments were performed on pooled ants from a single genetic background per replicate (Supplemental Table S16, r1 and r2). Replicate 3 was taken from a mixed genetic background (matched between castes and HS/control). For spike-in samples (second and third replicates), lysate from five *D. melanogaster* whole flies expressing *H. saltator* HSF1 or hsalHSF2 (10 flies total) was prepared in the same way as above (but in triple the volume) and then added to 5% of *H. saltator* lysate (as determined by Qubit high-sensitivity DNA reagents).

Production of custom antibodies Antibodies against *Harpegnathos* HSF1 (residues 240–500; accession no. XP_011144893.1) and hsalHSF2 (residues 105–240; accession no. XP_011141323.1) were raised against recombinant GST-tagged protein fragments. Rabbit immunization was performed by Cocalico Biologics. MBP-tagged versions of the same antigens were used for affinity purification from the resulting antisera. The antibodies were validated by immunoprecipitation Western blot (Supplemental Fig. S5B)

Fly crossing and rearing All overexpression crosses (Gal4 driver > UAS-hsalHSF1/hsalHSF2/dmHsf/nRFP) for heat shock survival, RNA-seq, and ChIP-seq were reared at 25°C and 50% humidity on a 12-h light/dark cycle using standard Bloomington *Drosophila* medium (Nutri-Fly) prior to heat stress or life span assessments. Day 0–1 F1 female flies were separated and reared in new vials. For aging assays, 10 female flies per vial were kept at either 25°C or 30°C with a 12-h light/dark cycle in vials with 5 mL of the standard Bloomington *Drosophila* medium (Nutri-Fly); 30°C was used to assess aging in the context of accelerated metabolic rate and stress (Morrow et al. 2004), and 25°C was used as the standard aging regime in *D. melanogaster* (Mołoń et al. 2020). Flies were flipped two to three times per week, and mortality was recorded. At least 10 vials (100 starting flies total) were used for each life span assay and condition to ensure reliable results.

For the long-term heat shock survival assay (Fig. 4A,B, right), 10 female flies (age 2–5 d) per vial were incubated for 24 h at 35.5°C, removing two vials every 4 h for 24 h. This was repeated for a total of three batches (six vials per time point per batch). For shorter heat shock survival assays, 10 female flies (age 2–5 d) per vial were incubated at the given temperature (Fig. 4), removed after heat shock, and incubated for 24 h at 25°C prior to assessment of survival. For all fly heat shock assays, vials for heat shock were first incubated for 1 h at the respective temperature to equalize vial temperatures prior to transfer of flies and incubation for the given duration at the given temperature.

Fly climbing assay

Fly climbing assay was performed mainly following a previous method (Ali et al. 2011). Surviving female flies at the given time point (d19 for elav-Gal4 crossed flies and d21 for PPL-Gal4 crossed flies) indicated in Figure 4C were transferred to a new vial on the given day. Only vials of six or more remaining flies (of the initial 10) were used. Three taps were given to knock all flies in the chamber to the bottom. After 10 sec of climbing, the percentage of flies not passing the drawn line was recorded. This was repeated three times, and the median number of flies for each vial was recorded. After this, flies were returned to 30° C to complete the 30°C stressed aging assay shown in Figure 4C.

Fly RNA-seq and ChIP-seq samples

For RNA-seq and ChIP-seq, female F1 offspring of UAS overexpression lines crossed to PPL-Gal4 flies were separated at d0–1. At d10, heat shock and control experimental flies were transferred to fresh vials already at 42°C and returned to incubation for 30 min at 42°C. Following heat shock, flies were kept for 15 min of recovery at 25°C and then placed on ice along with control flies. For RNA-seq, a single whole female fly was used for each replicate, homogenized in TriPure (Sigma), followed by RNA precipitation and poly(A) selection for mRNA-seq.

For ChIP-seq samples, three whole mated female F1 offspring of UAS overexpression lines crossed to PPL-Gal4 flies (age d10) were used. Immunoprecipitation was performed as described by Gospocic et al. (2021) but with the following modification: Sonication was performed in 1 mL using a Covaris S220 sonicator for 15 min (power: 140, duty factor: 5.0, cycles/burst: 200). ChIP-seq libraries were prepared as for those from ant tissues (described above).

Statistical analyses

Assignment of gene orthology and functional terms Using the reciprocal best BLAST hit method (Moreno-Hagelsieb and Latimer 2008), genes (NCBI *H. saltator* NCBI annotation release 102; assembly v 8.5) were assigned orthology to both *D. melanogaster* (r6.16) and *H. sapiens* (GRCh38) protein coding genes. These corresponding relationships are shown in Supplemental Table S1 of Gospocic et al. (2021).

GO terms were assigned to genes using the blast2go tool (Conesa et al. 2005) using the nr database, as well as InterPro domain predictions. GO enrichment tests were performed with the R package topGO (Alexa and Rahnenführer 2009), using Fisher's elimination method, and the resulting significant terms were entered into REVIGO (Supek et al. 2011) for collapsing of redundant terms.

RNA-seq analysis Reads were demultiplexed using bcl2fastq2 (Illumina) with the options "–mask-short-adapter-reads 20 –minimum-trimmed-read-length 20 –no-lane-splitting –barcode-mismatches 0." Reads were aligned to the *H. saltator* v8.5 assembly (Shields et al. 2018) using STAR (Dobin et al. 2013). STAR alignments were performed in two passes, with the first using the options "–outFilterType BySJout –outFilterMultimapNmax 20 –alignSJoverhangMin 7 –alignSJDBoverhangMin 1 –outFilterMismatchNmax 999 –outFilterMismatchNoverLmax 0.07 –alignIntronMin 20 –alignIntronMax 100000 –alignMatesGapMax 250000" and the second using the options "–outFilterType BySJout –outFilterMultimapNmax 20 –alignSJoverhangMin 8 –alignSJDBoverhangMin 1 –outFilterMismatchNmax 999 –outFilterMismatchNoverLmax 0.04 –alignIntronMin 20 –alignIntronMax 500000 –alignMatesGapMax 500000 –sjdbFileChrStartEnd [SJ_files]," where "[SJ_files]" corresponds to the splice junctions produced from all first-pass runs.

Gene-level read counts were produced using featureCounts (Liao et al. 2014) with the options "-O -M –fraction -s 2 –p," against a custom adapted NCBI *Harpegnathos* annotation (see below). The resulting counts were rounded to integers prior to importing into R for DESeq2 analysis in order to account for fractional count values associated with fractional counting of multimapping reads.

Because we observed a large number of genes that possessed truncated 3′ UTRs in the *H. saltator* NCBI annotation relative to aligned brain RNA-seq data, we used modified gene annotations featuring extended 3′ UTRs, prepared as described in Gospocic et al. (2021).

Differential gene expression tests were performed with DESeq2 (Love et al. 2014). For all pairwise comparisons, the Wald negative binomial test (test = "Wald") was used for determining differentially expressed genes. For analyses of *H. saltator* RNA-seq data, genetic background was entered as a blocking variable to control for the effect of genetic background. For caste-specific changes with condition (e.g., caste-specific aging changes or caste-specific heat shock response changes in gene expression), the specific caste X condition was compared with all other samples in a given comparison after blocking for colony background and general caste effects. When testing for general heat shock, DEGs samples from both castes were used, comparing HS with control samples after blocking for caste. Unless otherwise stated, an adjusted *P*-value cutoff of 0.1 was used to define differentially expressed genes.

For the PCA in Figure 5B, in order to identify genes differing across samples in all contexts, we performed a likelihood ratio test in DESeq2 comparing the full model "~line + condition + line:condition" with the reduced model "~1." Genes with an adjusted *P*-value of <0.01 were used to perform a PCA on variance stabilizing transformed expression values.

For identification of heat shock response genes, genes annotated with the GO terms "response to heat" (GO: 0009408), "protein refolding" (GO: 0042026), "response to unfolded protein" (GO: 0006986), and "chaperone-mediated protein folding" (GO: 0061077) were examined, as were several DNAJ proteins annotated in model organisms that our own annotation missed.

ChIP-seq analysis Demultiplexed reads were trimmed using Trimmomatic (Bolger et al. 2014) with the options "ILLUMINACLIP:[adapter.fa]:2:30:10 LEADING:5 TRAILING:5 SLIDINGWINDOW:4:15 MINLEN:15," and aligned to the *Harpegnathos* v8.5 assembly (Shields et al. 2018) using bowtie2 v2.2.6 (Langmead et al. 2009) with the option "–sensitive-local." Alignments with a mapping quality <5 and duplicated reads were removed using SAMtools (Li et al. 2009), as were reads overlapping a custom set of blacklisted regions, produced as in Amemiya et al. (2019) using input sonication control samples from this study, as well as in Gospocic et al. (2021). Peaks were called using MACS2 v2.1.1.20160309 (Zhang et al. 2008) on paired-end data with the options "–call-summits –nomodel -B."

For determination of general peaks and HSF-bound genes (Figs. 2, 3; Supplemental Figs. S5, S6, S10), peaks were called in individual replicates, and a peak was retained if independently called in two or more replicates. For peak classification, promoters were defined as the region spanning 2 kb upstream of and 0.5 kb downstream from the transcription start site of a gene. Genes bound by HSFs were defined as those genes containing a "strong" (fold enrichment over input >3) ChIP-seq peak within the promoter.

Differential HSF ChIP peaks (Fig. 3; Supplemental Figs. S7, S10) were called using DiffBind (Ross-Innes et al. 2012) using the option "summits=250" in the dba.count() function and "bFullLibrarySize=FALSE, bSubControl=TRUE, bTagwise=FALSE" for dba.analyze(), and all peaks called by MACS2 were used regardless of fold enrichment. For comparisons where one condition largely lacked any peaks (e.g., heat shock vs. control samples, as well as hsalHSF2 caste-specific binding without heat shock), the option "bFullLibrarySize=TRUE" was used in order to avoid normalization artifacts arising from scaling of the background read counts in the unbound condition.

For DiffBind testing, the DESeq2 algorithm (Wald negative binomial test) with blocking was used, and ChIP replicate was used as the blocking factor while testing for caste differences. When comparing general heat shock versus control peaks, caste was used as a blocking factor. An adjusted *P*-value of 0.05 was used as the threshold to define differential binding. For DiffBind analyses, all peaks generated by MACS2 were used

To generate genome browser tracks and heat maps, RPM (reads per million) was calculated for each biological replicate and then averaged.

Statistics

Sample size and statistical tests are indicated in the figure legends, and a list of samples, replicates, and genotypes is in Supplemental Table S17. Unless otherwise noted, all statistical tests were two-sided. Box plots were drawn using default parameters in R (center line, median; box limits, upper and lower quartiles; whiskers, 1.5× interquartile range). For testing significance of gene overlaps, we used the GeneOverlap R package (https://bioconductor.statistik.tu-dortmund.de/packages/3.9/bioc/html/GeneOverlap.html) and the R package OrderedList (Lottaz et al. 2006). For comparisons given in box plots, nonparametric tests were used: Mann–Whitney *U*-tests were used for all one-way comparisons, and Kruskal–Wallis tests followed by Dunn's correction were used for comparisons between three or more groups.

Data availability

All sequencing data related to this project has been deposited in the NCBI SRA BioProject under accession number PRJNA876839.

Competing interest statement

The authors declare no competing interests.

Acknowledgments

We thank members of the Berger laboratory for help in editing the manuscript. This work was supported by National Institutes of Health training grant F32GM120933 (to K.M.G.), National Institute on Aging grants R01AG055570 (to S.L.B.) and R01AG071818 (to R.B.), and National Institute of Mental Health grants R21MH123841 (to R.B.) and R01MH131861 (to R.B.).

Author contributions: K.M.G., J.R., J.G., and S.L.B. designed the experiments. K.M.G. and J.R. collected the data. K.M.G. analyzed the data. J.G. provided technical support. K.M.G. and S.L.B. wrote the manuscript with input from all coauthors.

References

Åkerfelt M, Morimoto RI, Sistonen L. 2010. Heat shock factors: integrators of cell stress, development and lifespan. *Nat Rev Mol Cell Biol* **11:** 545–555. doi:10.1038/nrm2938

Alexa A, Rahnenführer J. 2009. Gene set enrichment analysis with topGO. *Bioconductor Improv* **27:** 1–26.

Ali YO, Escala W, Ruan K, Zhai RG. 2011. Assaying locomotor, learning, and memory deficits in *Drosophila* models of neurodegeneration. *J Vis Exp* **49:** e2504. doi:10.3791/2504

Amemiya HM, Kundaje A, Boyle AP. 2019. The ENCODE blacklist: identification of problematic regions of the genome. *Sci Rep* **9:** 1–5. doi:10.1038/s41598-019-45839-z

Arrese EL, Soulages JL. 2010. Insect fat body: energy, metabolism, and regulation. *Annu Rev Entomol* **55:** 207–225. doi:10.1146/annurev-ento-112408-085356

Baler R, Dahl G, Voellmy R. 1993. Activation of human heat shock genes is accompanied by oligomerization, modification, and rapid translocation of heat shock transcription factor HSF1. *Mol Cell Biol* **13:** 2486–2496. doi:10.1128/mcb.13.4.2486-2496.1993

Barna J, Princz A, Kosztelnik M, Hargitai B, Takács-Vellai K, Vellai T. 2012. Heat shock factor-1 intertwines insulin/IGF-1, TGF-β and cGMP signaling to control development and aging. *BMC Dev Biol* **12:** 1–12. doi:10.1186/1471-213X-12-32

Bolger AM, Lohse M, Usadel B. 2014. Trimmomatic: a flexible trimmer for Illumina sequence data. *Bioinformatics* **30:** 2114–2120. doi:10.1093/bioinformatics/btu170

Calderwood SK, Murshid A, Prince T. 2009. The shock of aging: molecular chaperones and the heat shock response in longevity and aging—a mini-review. *Gerontology* **55:** 550–558. doi:10.1159/000225957

Choi MR, Jung KH, Park JH, Das ND, Chung MK, Choi IG, Lee BC, Park KS, Chai YG. 2011. Ethanol-induced small heat shock protein genes in the differentiation of mouse embryonic neural stem cells. *Arch Toxicol* **85:** 293–304. doi:10.1007/s00204-010-0591-z

Conesa A, Gotz S, Garcia-Gomez JM, Terol J, Talon M, Robles M. 2005. Blast2GO: a universal tool for annotation, visualization and analysis in functional genomics research. *Bioinformatics* **21:** 3674–3676. doi:10.1093/bioinformatics/bti610

Dobin A, Davis CA, Schlesinger F, Drenkow J, Zaleski C, Jha S, Batut P, Chaisson M, Gingeras TR. 2013. STAR: ultrafast universal RNA-seq aligner. *Bioinformatics* **29:** 15–21. doi:10.1093/bioinformatics/bts635

Dukay B, Csoboz B, Tóth ME. 2019. Heat-shock proteins in neuroinflammation. *Front Pharmacol* **10:** 920. doi:10.3389/fphar.2019.00920

Ghaninia M, Haight K, Berger SL, Reinberg D, Zwiebel LJ, Ray A, Liebig J. 2017. Chemosensory sensitivity reflects reproductive status in the ant *Harpegnathos saltator*. *Sci Rep* **7:** 1–9. doi:10.1038/s41598-017-03964-7

Gifondorwa DJ, Robinson MB, Hayes CD, Taylor AR, Prevette DM, Oppenheim RW, Caress J, Milligan CE. 2007. Exogenous delivery of heat shock protein 70 increases lifespan in a mouse model of amyotrophic lateral sclerosis. *J Neurosci* **27:** 13173–13180. doi:10.1523/JNEUROSCI.4057-07.2007

Glastad KM, Graham RJ, Ju L, Roessler J, Brady CM, Berger SL. 2020. Epigenetic regulator CoREST controls social behavior in ants. *Mol Cell* **77:** 338–351.e6. doi:10.1016/j.molcel.2019.10.012

Gomez-Pastor R, Burchfiel ET, Thiele DJ. 2018. Regulation of heat shock transcription factors and their roles in physiology and disease. *Nat Rev Mol Cell Biol* **19:** 4–19. doi:10.1038/nrm.2017.73

Gospocic J, Shields EJ, Glastad KM, Lin Y, Penick CA, Yan H, Mikheyev AS, Linksvayer TA, Garcia BA, Berger SL, et al. 2017. The neuropeptide corazonin controls social behavior and caste identity in ants. *Cell* **170:** 748–759.e12. doi:10.1016/j.cell.2017.07.014

Gospocic J, Glastad KM, Sheng L, Shields EJ, Berger SL, Bonasio R. 2021. Kr-h1 maintains distinct caste-specific neurotranscriptomes in response to socially regulated hormones. *Cell* **184:** 5807–5823.e14. doi:10.1016/j.cell.2021.10.006

Hsu A-L, Murphy CT, Kenyon C. 2003. Regulation of aging and age-related disease by DAF-16 and heat-shock factor. *Science* **300:** 1142–1145. doi:10.1126/science.1083701

Ito K, Shinomiya K, Ito M, Armstrong JD, Boyan G, Hartenstein V, Harzsch S, Heisenberg M, Homberg U, Jenett A, et al. 2014. A systematic nomenclature for the insect brain. *Neuron* **81:** 755–765. doi:10.1016/j.neuron.2013.12.017

Jemielity S, Chapuisat M, Parker JD, Keller L. 2005. Long live the queen: studying aging in social insects. *Age* **27:** 241–248. doi:10.1007/s11357-005-2916-z

Kaushik S, Cuervo AM. 2015. Proteostasis and aging. *Nat Med* **21:** 1406–1415. doi:10.1038/nm.4001

Kawazoe Y, Tanabe M, Sasai N, Nagata K, Nakai A. 1999. HSF3 is a major heat shock responsive factor duringchicken embryonic development. *Eur J Biochem* **265:** 688–697. doi:10.1046/j.1432-1327.1999.00762.x

Keller L. 1998. Queen lifespan and colony characteristics in ants and termites. *Insectes Soc* **45:** 235–246. doi:10.1007/s000400050084

Kozeretska IA, Serga SV, Koliada AK, Vaiserman AM. 2017. Epigenetic regulation of longevity in insects. In *Advances in insect physiology, vol. 53* (ed. Verlinden H), pp. 87–114. Elsevier, London, UK.

Kramer BH, Schaible R. 2013a. Colony size explains the lifespan differences between queens and workers in eusocial Hymenoptera. *Biol J Linn Soc* **109:** 710–724. doi:10.1111/bij.12072

Kramer BH, Schaible R. 2013b. Life span evolution in eusocial workers—a theoretical approach to understanding the effects of extrinsic mortality in a hierarchical system. *PLoS One* **8:** e61813. doi:10.1371/journal.pone.0061813

Krebs R, Loeschcke V. 1994. Costs and benefits of activation of the heat-shock response in *Drosophila melanogaster*. *Funct Ecol* **8:** 730–737. doi:10.2307/2390232

Labbadia J, Morimoto RI. 2015. The biology of proteostasis in aging and disease. *Annu Rev Biochem* **84:** 435–464. doi:10.1146/annurev-biochem-060614-033955

Langmead B, Trapnell C, Pop M, Salzberg S. 2009. Ultrafast and memory-efficient alignment of short DNA sequences to the human genome. *Genome Biol* **10:** R25. doi:10.1186/gb-2009-10-3-r25

Li H, Handsaker B, Wysoker A, Fennell T, Ruan J, Homer N, Marth G, Abecasis G, Durbin R, Subgroup GPDP. 2009. The sequence alignment/map format and SAMtools. *Bioinformatics* **25:** 2078–2079. doi:10.1093/bioinformatics/btp352

Liang V, Ullrich M, Lam H, Chew YL, Banister S, Song X, Zaw T, Kassiou M, Götz J, Nicholas HR. 2014. Altered proteostasis in aging and heat shock response in *C. elegans* revealed by analysis of the global and de novo synthesized proteome. *Cell Mol Life Sci* **71:** 3339–3361. doi:10.1007/s00018-014-1558-7

Liao Y, Smyth GK, Shi W. 2014. featureCounts: an efficient general purpose program for assigning sequence reads to genomic features. *Bioinformatics* **30:** 923–930. doi:10.1093/bioinformatics/btt656

Lindquist S. 1986. The heat-shock response. *Annu Rev Biochem* **55:** 1151–1191. doi:10.1146/annurev.bi.55.070186.005443

Livak KJ, Schmittgen TD. 2001. Analysis of relative gene expression data using real-time quantitative PCR and the 2−ΔΔCT method. *Methods* **25:** 402–408. doi:10.1006/meth.2001.1262

Lottaz C, Yang X, Scheid S, Spang R. 2006. OrderedList—a Bioconductor package for detecting similarity in ordered gene lists. *Bioinformatics* **22:** 2315–2316. doi:10.1093/bioinformatics/btl385

Love M, Huber W, Anders S. 2014. Moderated estimation of fold change and dispersion for RNA-seq data with DESeq2. *Genome Biol* **15:** 550. doi:10.1186/s13059-014-0550-8

Martins R, Lithgow GJ, Link W. 2016. Long live FOXO: unraveling the role of FOXO proteins in aging and longevity. *Aging cell* **15:** 196–207. doi:10.1111/acel.12427

Mezger V, Rallu M, Morimoto RI, Morange M, Renard J-P. 1994. Heat shock factor 2-like activity in mouse blastocysts. *Dev Biol* **166:** 819–822. doi:10.1006/dbio.1994.1361

Mitchell HK, Moller G, Petersen NS, Lipps-Sarmiento L. 1979. Specific protection from phenocopy induction by heat shock. *Dev Genet* **1:** 181–192. doi:10.1002/dvg.1020010206

Mołoń M, Dampc J, Kula-Maximenko M, Zebrowski J, Mołoń A, Dobler R, Durak R, Skoczowski A. 2020. Effects of temperature on lifespan of *Drosophila melanogaster* from different genetic backgrounds: links between metabolic rate and longevity. *Insects* **11:** 470. doi:10.3390/insects11080470

Moreno-Hagelsieb G, Latimer K. 2008. Choosing BLAST options for better detection of orthologs as reciprocal best hits. *Bioinformatics* **24:** 319–324. doi:10.1093/bioinformatics/btm585

Morley JF, Morimoto RI. 2004. Regulation of longevity in *Caenorhabditis elegans* by heat shock factor and molecular chaperones. *Mol Biol Cell* **15:** 657–664. doi:10.1091/mbc.e03-07-0532

Morrow G, Tanguay RM. 2015. *Drosophila melanogaster* Hsp22: a mitochondrial small heat shock protein influencing the aging process. *Front Genet* **6:** 103. doi:10.3389/fgene.2015.00103

Morrow G, Samson M, Michaud SM, Tanguay R. 2004. Overexpression of the small mitochondrial Hsp22 extends *Drosophila* life span and increases resistance to oxidative stress. *FASEB J* **18:** 598–599. doi:10.1096/fj.03-0860fje

Östling P, Björk JK, Roos-Mattjus P, Mezger V, Sistonen L. 2007. Heat shock factor 2 (HSF2) contributes to inducible expression of hsp genes through interplay with HSF1. *J Biol Chem* **282:** 7077–7086. doi:10.1074/jbc.M607556200

Pérez VI, Buffenstein R, Masamsetti V, Leonard S, Salmon AB, Mele J, Andziak B, Yang T, Edrey Y, Friguet B, et al. 2009. Protein stability and resistance to oxidative stress are determinants of longevity in the longest-living rodent, the naked mole-rat. *Proc Natl Acad Sci* **106:** 3059–3064. doi:10.1073/pnas.0809620106

Qiu X-B, Shao Y-M, Miao S, Wang L. 2006. The diversity of the DnaJ/Hsp40 family, the crucial partners for Hsp70 chaperones. *Cell Mol Life Sci* **63:** 2560–2570. doi:10.1007/s00018-006-6192-6

Ross-Innes CS, Stark R, Teschendorff AE, Holmes KA, Ali HR, Dunning MJ, Brown GD, Gojis O, Ellis IO, Green AR, et al. 2012. Differential oestrogen receptor binding is associated with clinical outcome in breast cancer. *Nature* **481:** 389–393. doi:10.1038/nature10730

Salway KD, Gallagher EJ, Page MM, Stuart JA. 2011. Higher levels of heat shock proteins in longer-lived mammals and birds. *Mech Ageing Dev* **132:** 287–297. doi:10.1016/j.mad.2011.06.002

San Gil R, Ooi L, Yerbury JJ, Ecroyd H. 2017. The heat shock response in neurons and astroglia and its role in neurodegenerative diseases. *Mol Neurodegen* **12:** 1–20. doi:10.1186/s13024-017-0208-6

Sandqvist A, Björk JK, Åkerfelt M, Chitikova Z, Grichine A, Vourc'h C, Jolly C, Salminen TA, Nymalm Y, Sistonen L. 2009. Heterotrimerization of heat-shock factors 1 and 2 provides a transcriptional switch in response to distinct stimuli. *Mol Biol Cell* **20:** 1340–1347. doi:10.1091/mbc.e08-08-0864

Schneider SA, Schrader C, Wagner AE, Boesch-Saadatmandi C, Liebig J, Rimbach G, Roeder T. 2011. Stress resistance and longevity are not directly linked to levels of enzymatic antioxidants in the ponerine ant *Harpegnathos saltator*. *PLoS One* **6:** e14601. doi:10.1371/journal.pone.0014601

Sheng L, Shields EJ, Gospocic J, Glastad KM, Ratchasanmuang P, Berger SL, Raj A, Little S, Bonasio R. 2020. Social reprogramming in ants induces longevity-associated glia remodeling. *Sci Adv* **6:** eaba9869. doi:10.1126/sciadv.aba9869

Shields EJ, Sheng L, Weiner AK, Garcia BA, Bonasio R. 2018. High-quality genome assemblies reveal long non-coding RNAs expressed in ant brains. *Cell Rep* **23:** 3078–3090. doi:10.1016/j.celrep.2018.05.014

Shinkawa T, Tan K, Fujimoto M, Hayashida N, Yamamoto K, Takaki E, Takii R, Prakasam R, Inouye S, Mezger V, et al. 2011. Heat shock factor 2 is required for maintaining proteostasis against febrile-range thermal stress and polyglutamine aggregation. *Mol Biol Cell* **22:** 3571–3583. doi:10.1091/mbc.e11-04-0330

Soti C, Csermely P. 2003. Aging and molecular chaperones. *Exp Gerontol* **38:** 1037–1040. doi:10.1016/S0531-5565(03)00185-2

Supek F, Bošnjak M, Škunca N, Šmuc T. 2011. REVIGO summarizes and visualizes long lists of gene ontology terms. *PLoS One* **6:** e21800. doi:10.1371/journal.pone.0021800

Taylor RC, Dillin A. 2011. Aging as an event of proteostasis collapse. *Cold Spring Harb Perspect Biol* **3:** a004440. doi:10.1101/cshperspect.a004440

Vos MJ, Hageman J, Carra S, Kampinga HH. 2008. Structural and functional diversities between members of the human HSPB, HSPH, HSPA, and DNAJ chaperone families. *Biochemistry* **47:** 7001–7011. doi:10.1021/bi800639z

Vos MJ, Carra S, Kanon B, Bosveld F, Klauke K, Sibon OC, Kampinga HH. 2016. Specific protein homeostatic functions of small heat-shock proteins increase lifespan. *Aging cell* **15:** 217–226. doi:10.1111/acel.12422

Walker GA, Lithgow GJ. 2003. Lifespan extension in *C. elegans* by a molecular chaperone dependent upon insulin-like signals. *Aging cell* **2:** 131–139. doi:10.1046/j.1474-9728.2003.00045.x

Wang H-D, Kazemi-Esfarjani P, Benzer S. 2004. Multiple-stress analysis for isolation of *Drosophila* longevity genes. *Proc Natl Acad Sci* **101:** 12610–12615. doi:10.1073/pnas.0404648101

Wang J-W, Beck ES, McCabe BD. 2012. A modular toolset for recombination transgenesis and neurogenetic analysis of *Drosophila*. *PLoS One* **7:** e42102. doi:10.1371/journal.pone.0042102

Waterhouse RM, Zdobnov EM, Tegenfeldt F, Li J, Kriventseva EV. 2011. OrthoDB: the hierarchical catalog of eukaryotic orthologs in 2011. *Nucleic Acids Res* **39:** D283–D288. doi:10.1093/nar/gkq930

Xie Y, Calderwood S. 2001. Transcriptional repression by heat shock factor 1. *Curr Top Biomed Res* **4:** 81–88.

Yan H, Opachaloemphan C, Carmona-Aldana F, Mancini G, Mlejnek J, Descostes N, Sieriebriennikov B, Leibholz A, Zhou X, Ding L, et al. 2022. Insulin signaling in the long-lived reproductive caste of ants. *Science* **377:** 1092–1099. doi:10.1126/science.abm8767

Zhang C, Cuervo AM. 2008. Restoration of chaperone-mediated autophagy in aging liver improves cellular maintenance and hepatic function. *Nat Med* **14:** 959–965. doi:10.1038/nm.1851

Zhang Y, Liu T, Meyer CA, Eeckhoute J, Johnson DS, Bernstein BE, Nussbaum C, Myers RM, Brown M, Li W, et al. 2008. Model-based analysis of ChIP-seq (MACS). *Genome Biol* **9:** R137. doi:10.1186/gb-2008-9-9-r137

Zhong S, Joung JG, Zheng Y, Chen YR, Liu B, Shao Y, Xiang JZ, Fei Z, Giovannoni JJ. 2011. High-throughput illumina strand-specific RNA sequencing library preparation. *Cold Spring Harb Protoc* **2011:** pdb.prot5652. doi:10.1101/pdb.prot5652